Morphometric analysis of subcortical structures in progressive supranuclear palsy: In vivo evidence of neostriatal and mesencephalic atrophy

Looi, Jeffrey C. L.; Macfarlane, Matthew D.; Walterfang, Mark; Styner, Martin; Velakoulis, Dennis; Latt, Jimmy; van Westen, Danielle; Nilsson, Christer

Published in:
Psychiatry Research: Neuroimaging

DOI:
10.1016/j.pscychresns.2011.07.013

2011

***Title Page showing full Author and Address Details**

Morphometric analysis of subcortical structures in Progressive Supranuclear Palsy: in vivo evidence of neostriatal and mesencephalic atrophy

[Word count 5221 – (Text Including Citations), Abstract 228, References 1553]

Authors:

Jeffrey Chee Leong Looi[a*†]; Matthew D. Macfarlane[a*]; Mark Walterfang[b*]; Martin Styner[c], Dennis Velakoulis[b], Jimmy Lätt[d]; Danielle van Westen[d, e]; Christer Nilsson[f]

Affiliations

a) Research Centre for the Neurosciences of Ageing, Academic Unit of Psychological Medicine, School of Clinical Medicine, Australian National University Medical School, Canberra, Australia
b) Melbourne Neuropsychiatry Centre, Royal Melbourne Hospital and University of Melbourne, Melbourne, Australia
c) Department of Psychiatry and Department of Computer Science, University of North Carolina, Chapel Hill, North Carolina, USA
d) Center for Medical Imaging and Physiology, Skåne University Hospital, Lund, Sweden
e) Diagnostic Radiology, Department of Clinical Sciences, Lund University, Lund, Sweden
f) Geriatric Psychiatry, Department of Clinical Sciences, Lund University, Lund, Sweden

*Equal first co-authors – we assert that the first three authors contributed equally as first co-authors

† Correspondence:

Associate Professor Jeffrey Looi

Academic Unit of Psychological Medicine

ANU Medical School

Building 4, Level 2, Canberra Hospital

Garran A.C.T. 2605

Email: jeffrey.looi@anu.edu.au

Abstract

Progressive supranuclear palsy (PSP) is a neurodegenerative disease characterized by gait and postural disturbance, gaze palsy, apathy, decreased verbal fluency and dysexecutive symptoms, with some of these clinical features potentially having origins in degeneration of frontostriatal circuits and the mesencephalon. This hypothesis was investigated by manual segmentation of the caudate and putamen on MRI scans, using previously published protocols, in 15 subjects with PSP and 15 healthy age-matched controls. Midbrain atrophy was assessed by measurement of mid-sagittal area of the midbrain and pons. Shape analysis of the caudate and putamen was performed using spherical harmonics (SPHARM-PDM, University of North Carolina). The sagittal pons area/midbrain area ratio (P/M ratio) was significantly higher in the PSP group, consistent with previous findings. Significantly smaller striatal volumes were found in the PSP group – putamina were 10% smaller and caudate volumes were 17% smaller than in controls after controlling for age and intracranial volume. Shape analysis revealed significant shape deflation in PSP in the striatum, compared to controls; with regionally significant change relevant to frontostriatal and corticostriatal circuits in the caudate. Thus, in a clinically diagnosed and biomarker-confirmed cohort with early PSP, we demonstrate that neostriatal volume and shape are significantly reduced *in vivo*. The findings suggest a neostriatal and mesencephalic structural basis for the clinical features of PSP leading to frontostriatal and mesocortical-striatal circuit disruption.

Keywords: Neostriatum, Caudate, Putamen, Mesencephalon, Magnetic Resonance Imaging,

1. Introduction

Progressive supranuclear palsy (PSP) is a neurodegenerative disorder characterized by postural instability and gait disturbance, bradykinesia and axial rigidity, vertical gaze palsy and bulbar palsy (Steele et al., 1964), in combination with neuropsychiatric symptoms such as apathy and utilization behaviour. Cognitive and behavioral features in PSP involve functional domains ascribed neuroanatomically to the fronto-striato-pallido-thalamic-cortical (frontostriatal) re-entrant circuits (Alexander et al., 1986; Cummings, 1993). PSP has a progressive and irreversible course, with disease duration usually between 6-12 years (Williams and Lees, 2009).

The molecular pathology of PSP is characterized by accumulation of tau protein and neuropil filaments within the pallidum, subthalamic nucleus, red nucleus, oculomotor nucleus, dentate nucleus, medulla, ventral tegmentum and neostriatum (caudate and especially putamen) (Williams and Lees, 2009). Macroscopic atrophy of the frontal cortex (Cordato et al., 2002) and subcortical structures (Schulz 1999; Schrag et al., 2000) distinguishes PSP from other parkinsonian syndromes on MRI. Subcortical atrophy in PSP affects the midbrain (particularly the ventral tegmentum), neostriatum, mamillary bodies and the superior cerebellar peduncle (Schrag et al., 2000), with the neostriatum and midbrain involved in frontostriatal circuits. Hence, there is morphological evidence that frontostriatal pathways may be disrupted by PSP.

Given the strategic location of the neostriatum in frontostriatal circuits, there have been surprisingly few attempts to quantify neostriatal atrophy as a structural basis for the neuropsychiatric clinical features of PSP. A post-mortem study of four patients with PSP found non-significant reductions in the cross-sectional area of striatal structures (Mann et al., 1993). Another small (n=6) MRI study found significant

reductions in striatal volume in PSP patients (Schulz et al., 1999). Cordato et al. (2002) identified 15% reduction in caudate volume (normalized for intracranial volume) in a PSP sample (n=21), but this was not significant once corrected for whole brain size. The Schulz et al. (1999) study is therefore the only study to our knowledge that has successfully quantified previously pathologically observed striatal atrophy in PSP *in vivo*.

Previous morphometric research has demonstrated that neostriatal shape and volume change *in vivo*, assessed via MRI, is apparent in neurodegenerative disease that involves fronto- or cortico-striatal neuronal circuits such as frontotemporal lobar degeneration and subtypes, Alzheimer's disease, and choreoacanthocytosis (Looi et al., 2010: Looi et al., 2011; Madsen et al., 2010; Walterfang et al., 2011). The neuroanatomical correlates of such research yield volume and shape. Form or shape is closely related to function (Thompson, 1945), and deformity to dysfunction in the neostriatum (Looi et al., 2010: Looi et al., 2011; Madsen et al., 2010; Walterfang et al., 2011). Medium size densely spiny projection neurons comprise 90-95% of the neostriatum and virtually all the cortical mantle projects as inputs to the neostriatum in a highly topographic pattern (Bolam et al., 2000). In turn, the output projections are directly to substantia nigra pars compacta and globus pallidus interna, and indirectly to globus pallidus externa (Bolam et al., 2000). In addition, the ventral tegmental area and substantia nigra pars compacta, both located in the midbrain, provide dopaminergic inputs to the neostriatum (Fields, 2007; Utter and Basso, 2008). Thus, the neostriatum serves as a topographically organized map of its cortical and subcortical connections (Haber, 2003; Draganski et al., 2008). Based upon the previous findings of neuropathologic and *in vivo* striatal atrophy in PSP and other neurodegenerative disease, we hypothesized that altered neostriatal morphology should be evident in PSP.

Previous clinical neuroimaging studies have confirmed the diagnostic accuracy of the 'penguin' or colibri (hummingbird) MRI sign of mesencephalic atrophy (Schrag et al., 2000) which has been quantified by decreased pons area/midbrain area ratio from a mid-sagittal MRI image (Oba et al., 2005; Quattrone et al., 2008). Named for the silhouette appearance of the pons and atrophic midbrain as a 'standing penguin' in cases of PSP, this sign may serve as a useful *in vivo* biomarker (see Fig 1). Mesencephalic atrophy may also lead to meso-cortical and meso-striatal disconnection, resulting in further frontostriatal dysfunction (Ikemoto, 2007; Fields, 2007; Sesack and Grace, 2010).

Given the implications of frontostriatal circuits, mesencephalic and neostriatal atrophy in the ætiopathology of PSP, and, as dysfunction arises from deformation, we hypothesized that altered neostriatal morphology should be evident in PSP. Our primary aim in this study was to perform morphometric analysis on neostriatal structures in order to quantify differences between patients with PSP and healthy age-matched controls measured as volume and shape of the caudate and putamen. Secondly, we hypothesized that subcortical mesencephalic atrophy would be evident through quantitative assessment of the penguin sign, and thus would serve as a confirmatory biomarker of PSP (Oba et al., 2005; Quattrone et al., 2008).

2. Method

2.1 Participants

Fifteen patients with progressive supranuclear palsy (PSP) were recruited for the study, representing an expanded cohort (patients and controls) of a previous study (Kvickström et al., 2011). The diagnosis of probable PSP was made using established clinical criteria (Litvan et al., 2003) in combination with clinical

investigations. The presence of fronto-subcortical symptoms (grouped into three categories: dysexecutive symptoms, apathy/lack of initiative and personality change) were recorded on the basis of clinical examination, review of medical records and interview with a caregiver. Disease severity was characterized by the Schwab and England (1969) scale for Parkinson's disease. The patients were followed up for an average of three years (range 2-5), to improve the accuracy of the clinical diagnosis. All MRI scans were performed a maximum of four years after symptom onset according to patient and caregiver interview. Fifteen healthy age-matched controls, assessed via interview and clinical examination, were recruited for comparison. Patients and controls were recruited from Lund University Hospital and Landskrona Hospital, Sweden. All patients and controls gave written consent to participate in the study, which was approved by the Regional Ethics Committee for Research.

2.2 Image Analysis

MRI was performed using a 3.0 T Philips MR scanner, equipped with an eight-channel head coil (Philips Achieva®, Philips Medical Systems, Best, The Netherlands). High resolution anatomical images were acquired using a T1-weighted turbo field echo (T1 TFE) pulse sequence with parameters set as follows: TR 8 ms; TE 4 ms; TI 650 ms; FA 10º; NEX 2; SENSE-factor 2.5; matrix 240 x 240; FOV 240; resulting voxel size 1 x 1 x 1 mm^3. In total 175 contiguous coronal slices were obtained. T2 FLAIR (TR / TE / TI / voxel size : 12000 msec / 140 msec / 2850 / 0.63 mm x 0.83 mm x 5 mm) and diffusion weighted (TR / TE / b-values / voxel size : 2255 ms / 55 ms/ b= 0, 1000 / 0.9 mm x 0.9 mm x 5 mm) images were used to assess the presence of focal lesions in the caudate nucleus and the putamen.

The T1-weighted images were anonymized, randomly coded to ensure blinding, and transferred to a MacBook Pro (Apple Inc, Cupertino, California, USA) computer at the Australia National University Medical School in Canberra, Australia.

Manual segmentation of striatal structures and area measurement (P/M ratio) was performed by a single investigator (MM) who was blind to clinical diagnosis for all measurements. Reliability of image analysis was performed by measuring intra-class correlations between initial segmentation and random repeated segmentation of five subjects, and was calculated in SPSS 17.0 (IBM Corporation, Somers, New York, USA). Inter-rater reliability of manual segmentation was also calculated from a second experienced tracer (JCLL).

2.2.1 Mid-sagittal pons and midbrain area

Quantification of mesencephalic atrophy was performed by measuring the area of the midbrain and pons in the mid-sagittal slice for each subject using ANALYZE 10.0b, by manual segmentation using a published protocol (Oba et al., 2005; Quattrone et al., 2008). Using these measures, we calculated the ratio of pons area to midbrain area (P/M ratio) (Figure 1).

Insert Figure 1 about here

2.2.2 Striatal Volumetric Analysis

Volumetric analysis was performed on the caudate nucleus and putamen bilaterally according to previously published protocols (Looi et al., 2008, 2009). Briefly, this involved using ANALYZE 10.0b (Mayo BIR, Rochester, New York, USA) to manually trace the outline of the caudate nucleus and putamen bilaterally through successive axial slices, in this series with reference to sagittal and coronal views, editing as required in orthogonal planes, and measuring the volume thus delineated. The tail of

the caudate and the nucleus accumbens below the axial plane of the inferior aspect anterior commissure were not included in the segmentations (Figure 2).

Insert Figure 2 about here

2.2.3 Intracranial volume measurement

The intracranial volume (ICV) was determined in a semi-automated fashion using FSL software (FMRIB Group, Oxford). First, brains were skull-stripped with the Brain Extraction Tool (BET) and were then linearly aligned to the MNI152 1mm T1-weighted template. The inverse of the determinant of the affine transformation matrix was multiplied by the ICV of the MNI152 template to produce a measure of ICV for use as a scaling factor, measured in cubic centimetres (ENIGMA, 2011).

2.3 Statistical analysis for volumetric and area measurements

Statistical analysis was performed using SPSS 17.0. Demographics were assessed using an independent-samples t-test, with gender distribution (equal proportions expected) assessed via Chi-square analysis. Intra-rater reliability (intra-class correlation coefficients, two-way mixed effects model for absolute agreement for all analyses) were used to assess reliability for manual striatal segmentation and measurement of PM ratio. Multivariate analysis of co-variance (MANCOVA) was used to assess the significance of any differences in bilateral caudate volume and bilateral putamen volume (bilateral volumes were used, as due to sample size and unequal errors of variance, full analyses by right and left side could not be performed using a MANCOVA) between the PSP and control groups; and between midbrain and pontine mid-sagittal area. Covariates were age and ICV. A receiver-operating characteristics (ROC) analysis was conducted to determine group membership, controls versus PSP, based upon bilateral caudate and bilateral putamen volume; and based upon P/M ratio. A univariate analysis of covariance (ANCOVA) was

performed on the differences in P/M ratio between the PSP and control groups. Checks of assumption of normality, linearity, homogeneity of variances/regression slopes and reliable measurements of covariates were performed prior to the MANCOVA and ANCOVA. We performed partial correlations of striatal volumes and mid-sagittal pons/midbrain areas.

2.4 Shape analysis

Shape analysis was undertaken in a semi-automated fashion using the University of North Carolina shape analysis toolkit (http://www.nitrc.org/projects/spharm-pdm/); a detailed description of the methodology is available in (Styner et al., 2006; Levitt et al., 2009 - See Appendix A for detailed summary). Segmented 3D binaries are initially processed to ensure interior holes are filled, followed by morphological closing and minimal smoothing. These are then subjected to spherical harmonic shape description (SPHARM), whereby boundary surfaces of each shape are mapped onto the surface of a sphere and the surface coordinates were represented through their spherical harmonic coefficients (Brechbuhler et al., 1995). The correspondence between surfaces is established by parameter-based rotation, itself based on first-order expansion of the spherical harmonics. The surfaces are uniformly sampled into a set of 1002 surface points and aligned to a study-averaged template for each structure (left and right caudate and putamen) using rigid-body Procrustes alignment (Bookstein, 1997). Scaling normalization was performed to remove the effect of head size/intracranial volume, surface scaling factor: f_i, where $f_i = (\text{Mean}(ICV)/ICV_i)^{1/3}$ (Styner et al., 2007).

2.4.1 Shape statistical analyses

We compute non-parametric statistical tests that compare the local surface coordinates for group mean differences at the 1002 surface locations (Styner et al., 2006; Styner et al., 2007; Levitt et al., 2009). A local group difference metric between

groups of surface coordinates is derived from the Hotelling T^2 two sample metric (Styner et al., 2007). As the shape analysis involves computing 1002 hypothesis tests, one per surface location, a correction for multiple testing is necessary, as an uncorrected analysis would be overly optimistic. The shape analysis uses permutation tests of the Hotelling T^2 metric for the computation of the raw uncorrected *p*-values and false discovery rate (FDR) (Genovese et al., 2002) for multiple comparison correction.

The non-parametric, permutation-based approach is a way of managing multiple comparisons where data points are adjacent, or are non-independent in any way. Permutation-based analyses are used in shape analyses as this type of analysis invariably involve multiple measures of the same structure, and this method allows for multiple methods for controlling the multiple-comparison problem by controlling the false discovery rate, such as used in this study, or the family-wise error rate, in addition to allowing for analysis of a range of statistics also used in parametric tests such as F or t and allowing for alignment with parametric tests used elsewhere for non-shape based variables.

Shape statistical analysis significance maps showing local statistical p-values, raw and corrected for FDR, are generated. A global shape difference is computed, summarizing average group differences across the surface. Statistical shape analysis also provides visualizations of the local effect size via mean difference magnitude displacement maps, which display the magnitude of surface change (deflation or inflation) in mm between corresponding points on the mean surfaces of group 1 and group 2. The color scale of the magnitude displacement visualizations varies due to the different degrees of deflation in individual comparisons (e.g. PSP versus controls), with greater degrees of deflation requiring some compression of the color scale. In terms of absolute magnitude of displacement of the surface (mm) (mean

difference displacement maps), the groups may show differences; whilst on a point-wise surface comparison between the groups this displacement may not be statistically significant (statistical shape analysis significance map).

3. Results

3.1 Participants

The participants did not significantly differ with respect to age, gender and ICV *(Table 1)*. The T2 FLAIR sequence showed a focal, 5 x 3 mm large area of increased T2-signal in the anterior putamen on the left side in one PSP patient, most probably representing gliosis; this area did not reveal itself on the T1-weighted sequence. Otherwise no focal abnormalities were present on the caudate nucleus and putamen in the remaining patients or controls. Clinical details on severity of symptoms and neuropsychiatric measures for the PSP patients are included in Table 2. Seven of the fifteen patients had mild disease severity (Schwab and England disability score of 60-80%), the remainder had moderate-to-severe disease severity. Nine of the fifteen patients had at least one fronto-subcortical symptom.

Table 1 & 2 about here

3.11 Reliability Analysis

Intra-rater reliability (intra-class correlation coefficients, two-way mixed effects model for absolute agreement for all analyses) for manual striatal segmentation (20 measurements) was 0.95 for caudate volumes, 0.93 for putamen and inter-rater reliability was 0.89. Intra-rater reliability (20 measurements) for the P/M ratio was 0.94 on and inter-rater reliability was 0.998.

3.2 Tests of Between-Groups Effects in Striatal Structures (Table 3, Figure 3)

The mean volume of the bilateral caudate nuclei (right plus left) was 17.4% smaller in the PSP group compared to controls – 5207 mm^3 *versus* 6305 mm^3 (F=4.368, *P*=0.013). The mean volume of the bilateral putamen was 10.1% smaller in the PSP group compared to the control group – 4735 mm^3 *versus* 5267 mm^3 (F=3.695, df=3, *P*=0.024). A scatter-plot of bilateral caudate and putamen volume by group (Figure 3) shows that two-thirds (10 of 15) of PSP patients have bilateral caudate volume below 6000 mm^3, and bilateral putamen volume below 5500 mm^3.

A ROC analysis (Figure 4) was conducted to determine group membership based on bilateral caudate and bilateral putamen volume, showing that bilateral caudate volume of less than 5525 mm^3 predicted PSP membership versus control with a sensitivity of 0.933 and specificity 0.667, with area under the curve 0.796 +/- 0.084, asymptotic significance 0.006. The bilateral putamen volume was not significant in predicting PSP membership versus control. (See Appendix B for details of ROC analysis).

Table 3 about here, Figures 3-4 about here

3.3 Between-Groups Analysis of P/M Values (Table 3, Figure 5)

The raw midbrain and pontine mid-sagittal areas for PSP and controls are displayed in Table 2 and as a scatter plot in Figure 4. Midbrain area was significantly smaller in PSP compared to the control subjects (F=16.205, df=3, *P*<0.0001), representing a 35% reduction in area. Pontine mid-sagittal area was not significantly different between PSP and controls. The scatter plot shows that for all but one control, there is a clear demarcation in midbrain area (less than 120 mm^2) in PSP.

Figure 5 about here

The ratio of pontine area to midbrain area on mid-sagittal section was significantly higher in the PSP group. The mean P/M ratio in the PSP group was significantly higher in the PSP group compared to the control group (5.77 *vs* 3.99 ; *P*<0.01) (Please see Appendix C for details of further analyses for P/M ratio).

3.4 Within-groups partial correlational analysis of volumetry and midbrain/pons areas

Analysing partial correlations between volumetric and area measures, we found that bilateral caudate and putamen volume was significantly correlated in PSP, r= 0.791, *P*=0.001, but not in controls. When we analysed the PSP group by side, we found that the partial correlation held for all but the left putamen – right caudate: thus, right caudate and putamen, r=0.762, *P*=0.002; left caudate and right putamen, r=0.842, *P*<0.001; and left caudate and putamen, r=0.787, *P*=0.001. There were no other significant partial correlations between striatal volumes or mid-sagittal pons/midbrain areas.

3.5 Between-Groups Shape Analysis (Figure 6)

3.5.1 Shape analyses

We applied the shape analysis method to the segmented caudate and putamen for the entire dataset. All results were scaling normalized for total intracranial volume. The results presented are based upon FDR corrected *p*-value maps, together with corresponding local displacement maps. The details of the legend for the analyses are described below the images for ease of reference when reading the images (Figure 6).

3.5.2 Regional shape analysis and mean difference displacement results

These results are described with reference to the maps developed by Alexander et al., (1986), Haber (2003), Utter and Basso (2008), and Draganski et al. (2008), summarised in Figure 7. (See Figures 7-9)

Insert Figures 6-9 about here

3.5.2.1 Caudate

For the PSP group compared to controls, the left caudate shows significant regional shape deflation corresponding to the inputs from the following cortical areas: rostral motor, dorsolateral prefrontal cortex, anterior cingulate cortex, orbitofrontal cortex, and posteriorly, frontal eye fields, and caudal motor regions. The magnitude of deflation in the left caudate in PSP is marked, and of the order of several millimetres to tens of millimetres.

For the PSP group compared to controls, the right caudate shows relatively more significant regional shape deflation corresponding to the inputs from the following cortical areas: rostral motor, dorsolateral prefrontal cortex, orbitofrontal cortex, and posteriorly, frontal eye fields and caudal motor regions. The magnitude of deflation in the right caudate in PSP is less marked, and of the order of several millimetres only.

P-value of the average statistic across the whole surface for bilateral caudate is <0.05 indicating there is a significant overall shape change in the caudate for PSP compared to controls.

The bilateral caudate in PSP displays a number of orthogonal gradients of atrophy: dorsal to ventral; anterior to posterior; and lateral to medial.

3.5.2.2 Putamen

For the PSP group compared to controls, the bilateral putamen shows overall no significant regional shape deflation. However, the overall P-value of the average shape map statistic across the whole surface of right and left putamen is <0.05. The magnitude of general shape deflation bilaterally is of the order of 1-2 mm.

4. Discussion

We demonstrated that caudate and putamen volumes are significantly decreased *in vivo* (17.4% and 10.1% respectively) in patients with PSP, compared to controls. We also found global morphologic deflation of the neostriatum in the PSP group compared to controls, and significant regional atrophy in the bilateral caudate input regions from rostral motor, dorsolateral prefrontal cortex, anterior cingulate cortex, orbitofrontal cortex, frontal eye fields, and caudal motor regions. In addition, we quantified mesencephalic atrophy via mid-sagittal midbrain area, and the pontine-to-midbrain ratio in PSP, confirming the clinical diagnosis with an *in vivo* biomarker (Oba et al., 2005; Quattrone et al., 2008). The combination of quantified altered morphology of the neostriatum and mesencephalon in PSP indicates a strong neuroanatomical subcortical basis for the clinical features of PSP.

4.1 Mesencephalic morphometry

Midbrain atrophy in PSP has been quantified on structural MRI via different analysis methods. Using automated volumetry, one group demonstrated that midbrain atrophy was significant in PSP compared to controls (Gröschel et al., 2004). A voxel-based morphometric (VBM) study demonstrated that reduction in midbrain and pontine grey/white matter density was present in PSP compared to controls (Boxer et al., 2006), whilst another found reduced density in only thalamus and the colliculi, of the subcortical structures (Padovani et al., 2006).

Our study replicates the finding of Oba et al. (2005) and Quattrone et al. (2008) regarding the validity of the penguin/colibri sign, and confirms that mesencephalic atrophy can be significantly quantified in PSP compared to controls. The average midbrain mid-sagittal area in PSP was reduced by 35.5% compared to the area in controls. In our sample, the sensitivity of 86.7% and specificity of 93.3% for a cutoff of P/M 4.63 were similar to previous studies. This indicates that, in addition to satisfying established clinical criteria for PSP, subjects also had similar measurements to previous cohorts on an established biomarker for the disease. Other exploratory tests, looking for associations between mesencephalic area and striatal volumes, showed no significant correlation between the two sets of data. Mesencephalic atrophy may involve the substantia nigra, causing deafferentation and thus, dendritic degeneration of neostriatal medium spiny neurons, as has been demonstrated in Parkinson's disease (Zaja-Milatovic et al., 2005). Therefore, mesencephalic atrophy may result in altered neostriatal morphology.

4.2 Neostriatal morphometry

In previous *in vivo* neuroimaging, there have been studies suggesting altered neostriatal morphology in PSP. A previous structural MRI study with PSP (n=6) showed significant caudate and putaminal atrophy (Schulz et al., 1999). A study using manual segmentation of MRI in PSP (n=21) found a non-significant reduction of 15% in caudate volume, normalized to ICV, compared to controls, additionally controlling for whole brain volume (Cordato et al., 2002). A VBM study in 13 persons with PSP showed reduced grey matter density of caudate and midbrain (Josephs et al., 2008). A further VBM study demonstrated reduction in grey matter density in the caudate in 20 persons with PSP (Agosta et al., 2010); whilst magnetization transfer imaging showed a significant magnetization transfer ratio difference in the caudate and putamen in PSP versus controls, indicating neuronal structural changes in the disease (Eckert et al., 2004). Thus, our results are significant in quantifying the

morphology of *in vivo* atrophy in both caudate and putamen, and concurring with previous imaging findings.

The neostriatal atrophy we observed is consistent with neuropathologic findings that the tauopathy of PSP shows a predilection for the neostriatum (Daniel et al., 1995; Williams and Lees, 2009). Previous quantitative post-mortem neuropathologic studies of PSP have found putaminal atrophy (Oyanagi et al., 1994), whilst others have found similar degrees of caudate (10-15%) and putaminal atrophy (5-12%) to that which we found *in vivo* (Mann et al., 1993). Diffusion-weighted imaging in the putamen of patients with PSP (Seppi et al., 2003) has shown diffusion changes manifesting as an increased apparent diffusion coefficient (ADC), indicating loss of structural integrity of the putamen.

A number of studies have demonstrated neurophysiologic abnormalities in the neostriatum in PSP, and advanced hypotheses as to underlying pathology. The neurodegenerative changes in the striatum may result in a net loss of GABAergic neurons within the basal ganglia (Levy et al., 1995). There is a pronounced decrease in dopaminergic nerve terminals in the caudate and putamen of patients with PSP (Filippi et al., 2006), which may arise from loss of inputs from substantia nigra (Warren et al., 2007) and ventral tegmentum in the midbrain. Accordingly, the primary disease process in PSP may involve trans-synaptic degeneration from upstream or downstream brain regions within the neural network (van Buren, 1963), and thus be reflected in altered morphology of the highly interconnected neostriatum.

Interestingly, our partial correlation results suggest that the PSP disease process affects both caudate and putamen in parallel. From the ROC and shape analysis, the caudate is more clearly atrophic in PSP than the putamen. As the two structures are interconnected, atrophy in one may be correlated with the other.

The caudate and putamen are contiguous structures with differing functional specializations, such that the caudate is linked to frontal cortex serving executive, social and motivational cognition as well as frontal eye fields; whilst the putamen is linked to parietal cortex serving motor functions (Alexander et al., 1986; Haber, 2003; Draganski et al., 2008). Thus, atrophy of the neostriatum may serve as a structural basis for the dysexecutive syndrome, apathy, oculomotor dysfunction, obsessive-compulsive phenomena, and motor dysfunction observed clinically in PSP (Bak et al., 2010), through disruption of fronto-striato-pallido-thalamic or frontostriatal circuits, as has been previously observed in the neuroanatomically related disorders of frontotemporal lobar degeneration, Huntington's Disease and choreoacanthocytosis (Looi et al., 2010; Looi et al., 2011; Douaud et al., 2006; Walterfang et al., 2011).

Our morphometric results indicate possible structure-function relationships for the clinical manifestations of PSP. However, we acknowledge that clinical motor, emotional, behavior measurements, for correlation with the shape of the caudate and putamen, are needed to fully establish corticostriatal structure-function relationships.

4.2.1 Caudate morphometry

Our shape analysis (Figure 6) demonstrated significant regionally specific atrophy of the caudate in PSP that implicates loss of inputs/interconnections from frontal and parietal cortex, and by extension, mesencephalon. The patterns of regional shape deflation differ by hemisphere (see Figures 6-9). The left caudate shows more discrete, but nonetheless large magnitude shape deflations across the regions receiving inputs from: frontal cortex - dorsolateral prefrontal cortex, anterior cingulate cortex, orbitofrontal cortex; parietal cortex – rostral and caudal motor regions; frontal eye fields; and, possibly, via the ventral surface of the caudate/nucleus accumbens, ventral tegmentum and substantia nigra. In contrast, the right caudate shows almost

global atrophy of smaller magnitude, traversing regions corresponding to nearly all the interconnections of the caudate.

We found the following orthogonal atrophy gradients in the caudate: dorsal to ventral; anterior to posterior; and lateral to medial. Some of these gradients may arise from specific loss of inputs, such as the anterior to posterior pattern, may specifically impact on the nucleus accumbens neurogenic centre (Heimer and van Hoesen, 2006), and have been observed in other neurodegenerative diseases (Douad et al., 2006; Looi et al., 2010; Looi et al., 2011; Madsen et al., 2010; Walterfang et al., 2011). There is neuropathological evidence of selective dendritic degeneration in the medium spiny neurons (MSN) of the head of the caudate in dementia with Lewy Bodies (DLB) (Zaja-Milatovic et al., 2006) and evidence that neurogenesis occurs in the lateral but not rostral portions of the subventricular zone in animal models of Huntington's disease (Mazurová et al., 2006). The lateral-medial gradient of atrophy we observed in PSP may thus represent an impaired neurogenesis response to disease (Looi et al., 2010) in the subventricular zone (Curtis et al., 2007).

Caudate tauopathy in PSP may specifically damage the MSN, interneurons of circuits traversing the neostriatum, via dendritic degeneration similar to that seen in DLB (Zaja-Milatovic et al., 2006). The downstream effect of the deafferentation and dendritic degeneration in the MSN of the caudate may be reduced direct output to globus pallidus interna/substantia nigra pars compacta; resulting in reduced switching off of inhibitory pathways (Bolam et al., 2000) and thus, impersistence of cognitive functions, emotions, movements and behaviours carried by the corticostriatal circuits. Similarly, reduced indirect output to globus pallidus externa will impair feed-forward inhibitory pathways (Bolam et al., 2000). Therefore, the net result may be derailment of frontostriatal circuit mediated functions, such as the dysexecutive syndrome and apathy, combined with some loss of inhibition resulting

in aberrant autonomous behaviour such as stereotypies and obsessive-compulsive phenomena, all of which may be observed in PSP (Bak et al., 2010). There are also possible direct effects of caudate atrophy on oculomotor function (Utter & Basso, 2008) due to loss of interconnections to the frontal eye field (Looi et al., 2010).

4.2.2 Putamen morphometry

Although we found a significant reduction in bilateral putamen volume and found that overall right and left putamen shape was significantly different for persons with PSP compared to controls, the shape analysis revealed no regionally specific changes in putamen shape. The failure to show significant regional shape differences in the putamen may be an artefact of sample size, as the raw analyses showed some regional differences. The *P*-value of the average statistic across the surface was < 0.05, indicating that there was a significant overall shape deflation in PSP, which while not significant at any individual point, was 1-2 mm across the entire surface. Morphological change in PSP may have been more generalized and less regionally-specific in the putamen. Our previous shape analysis of the putamen in frontotemporal lobar degeneration (Looi et al., 2010) and choreoacanthocytosis (Walterfang et al., 2011) had larger numbers of control comparators, and thus may have had more power to resolve the perhaps lesser degree of alteration of morphology in the putamen. There is a significant reduction in volume and shape of the bilateral putamen with implications for the cortico-striatal circuits that traverse the putamen, including the frontostriatal circuits and links to premotor, motor cortex, somatosensory cortex, supplementary motor areas and frontal eye fields (Alexander et al., 1986; Utter and Basso, 2008). Accordingly, the altered general morphology of the putamen, combined with that of the caudate and mesencephalon may contribute to the structural basis of the bradykinesia, gait disturbance, oculomotor dysfunction and rigidity observed in PSP. Indeed, a recent VBM study has shown that putaminal

atrophy has been correlated with apathy as assessed using neuropsychiatric measures (Josephs et al., 2011)

4.3 Limitations

Definitive diagnosis of PSP requires autopsy. The positive predictive value of diagnosis via established clinical criteria varies between 78-91% in autopsy-confirmed series (Osaki et al., 2004). We therefore applied clinical criteria, together with clinical investigations and long-term follow-up to improve the accuracy of diagnosis. Our sample size, is small, although moderately sized in relation to previous volumetric neuroimaging studies in PSP. When we performed an exploratory MANCOVA of the striatal volumes by side, we found that unequal error variance precluded full analysis, and thus we opted for a MANCOVA of bilateral (combined right and left) striatal volume, deferring to the shape analysis to examine lateralized effects. Potentially there is heterogeneity in the degree of atrophy seen in the PSP group attributable to different symptom profiles and disease severity.

We used validated and reliable protocol for manual tracing, as opposed to automated segmentation. We acknowledge that tracing the images in the axial plane, albeit with reference to orthogonal views, may minimize differences in volume in this plane, and thus minimize differences between the groups overall. We used intracranial volume as a covariate (accepting that this is a proxy value for head size rather than brain volume) in the MANCOVA, and as a scaling factor in the shape analysis, allowing us to apply a consistent standard for normalization of the striatal volumes, as has been undertaken in similar volume/shape analysis papers (Looi et al., 2009; Looi et al., 2010; Looi et al., 2011; Walterfang et al., 2011).

We did not directly compare volumetrics and area measurements with previous neuroimaging studies as variations in diagnostic criteria, methodology and

demographics may contribute significantly to differences among studies. The failure to show significant regional shape differences in the putamen may be an artefact of sample size, and smaller group size can be a limitation when an excess of controls (twice or more the number of disease subjects) is not available. Generally, larger samples are required for a shape analysis than a volumetric analysis as the local effects are commonly smaller than the cumulative effect size across the whole structure. The ability to detect local differences depends on the effect size and sample size. Given that the caudate differences in volume were clearly larger than in putamen, it could be that the study was underpowered for showing differences in putamen, whilst it was well powered for showing differences in caudate shape. Indeed, we have occasionally found that some similarly sized comparisons have not survived the false-discovery rate correction in prior studies (Looi et al., 2011).

We are unaware of any accepted tracing protocols for volumetry of mesencephalic structures, which limited our investigation of this area to the mid-sagittal area measurement only – analyses of relationships between the mesencephalon and neostriatum may have been more fruitful if volumetry and shape analysis were feasible for the midbrain and pons.

4.4 Conclusion

In conclusion, we have found that significant neostriatal and mesencephalic atrophy is evident in mild-moderate PSP, in contrast to healthy age-matched controls. Via morphometric analysis, this atrophy has been demonstrated to map to regional interconnections from cortex and mesencephalon. The resultant disruption in frontostriatal and mesocortical circuits potentially provides a structural basis for the neuropsychiatric manifestations of PSP, such as the dysexecutive syndrome, gaze palsy, obsessive-compulsive phenomena and utilization behavior. Similarly, the structural basis of the movement disorders of PSP, bradykinesia, gait disturbance

and rigidity, potentially arises, at least in part, from altered morphology of the neostriatum and mesencephalon. Future prospective studies with larger cohorts, of potential neural networks affected in PSP, should focus on connections between the ventral tegmentum, the striatum and the frontal cortex, as well as correlations with clinical features such as cognitive, motor and behavioral measurements. Such studies may further demonstrate structural-functional correlations of striatal shape and clinical features.

We have descried multum in parvo*, via the neostriatum and the mesencephalon, a miniature chart of neuronal atrophy in progressive supranuclear palsy*.

Contributors

JCLL designed, coordinated and is guarantor of the study, performed image and statistical analysis, and co-authored the first draft of the paper. MM performed all measurements on striatal volumes and the P/M ratios, performed statistical analysis and co-authored the first draft of the paper. MW coordinated and performed the spherical harmonic shape analysis, automated analysis to determine intracranial volume, and co-authored the first draft of the paper. The first three authors assert they are equal first co-authors of the paper on the basis of their contributions. MS designed SPHARM-PDM tools and assisted with analysis DV is a co-investigator with MW and provided image analysis infrastructure. JL and DvW performed image pre-processing. DvW read the MRI for morphological findings. CN was responsible for recruitment and diagnosis of patients and controls, and is the principal investigator. All authors contributed to the writing of the final paper.

Acknowledgments

J.C.L. Looi self-funded travel expenses to develop this study with collaborators at Lund University and Skåne University Hospital, Lund, Sweden, with support from Lund University for accommodation expenses. M. Styner acknowledges the National Alliance for Medical Image Computing (NA-MIC) NIH U54 EB005149. This study was funded through grants from the Swedish Parkinson Fund and the Swedish Science Council (through the Basal Ganglia Disease Linnæus Consortium).

References

Alexander, G.E., Delong, M.R., Strick, P.L., 1986. Parallel organisation of functionally segregated circuits linking basal ganglia and cortex. Annual Review of Neuroscience 9, 357-381.

Agosta, F., Kostic, V.S., Galantucci, S., Mesaros, S., Svetel, M., Pagani, E., Stefanova, E., Filippi, M., 2010. The in vivo distribution of brain tissue loss in richardson's syndrome and PSP-parkinsonism: a VBM-DARTEL study. European Journal of Neuroscience 32, 640-647.

Bak, T.H., Crawford, L.M., Berrios, G., Hodges, J.R., 2010. Behavioural symptoms in progressive supranuclear palsy and frontotemporal dementia. Journal of Neurology Neurosurgery and Psychiatry 81, 1057-1059.

Bookstein, F.L., 1997. Shape and the information in medical images: a decade of the morphometric synthesis. Computer Vision and Image Understanding 66, 97–118.

Bolam, J.P., Hanley, J.J., Booth, P.A.C., Bevan, M.D., 2000. Synaptic organisation of the basal ganglia. Journal of Neuroanatomy 196, 527-542.

Boxer, A.L., Geschwind, M.D., Belfor, N., Gorno-Tempini, M.L., Scahuer, G.F., Miller, B.L., Weiner, M.W., Rosen, H.J., 2006. Patterns of brain atrophy that differentiate corticobasal degeneration syndrome from progressive supranuclear palsy. Archives of Neurology 63, 81-86.

Brechbuhler, C., Gerig, G., Kubler, O., 1995. Parametrization of closed surfaces for 3-D shape description. Computer Vision, Graphics, Image Processing 61,154–170.

Cordato, N.J., Pantelis, C., Halliday, G.M., Velakoulis, D., Wood, S.J., Stuart, G.W., Curries, J, Soo, M., Olivieri, G., Broe, G.A., Morris, J.G.L., 2002. Frontal atrophy correlates with behavioural changes in progressive supranuclear palsy. Brain 125, 789-800.

Cummings, J.L., 1993. Frontal subcortical circuits and human behaviour. Archives of Neurology 5, 873-880.

Curtis, M.A., Faull, R.L.M., Eriksson, P.S., 2007. The effect of neurodegenerative diseases on the subventricular zone. Nature Reviews Neuroscience 8, 712-723.

Daniel, S.E., de Bruin, V.M.S., Lees, A.J., 1995. The clinical and pathological spectrum of Steele-Richardson-Olszewski syndrome: progressive supranuclear palsy: a reappraisal. Brain 118, 759-770.

Draganski, B., Kherif, F., Kloppel, S., Cook, P.A., Alexander, D.C., Parker, G.J.M., Deichmann, R., Ashburner, J., Frackowiak, R.S.J., 2008. Evidence for segregated and integrative connectivity patterns in the human basal ganglia. Journal of Neuroscience 28, 7143-7152.

Douaud, G., Gaura, V., Ribeiro, M-J., Lethimonnier, F., Maroy, R., Verny, C., Krystkowiak, P., Damier, P., Bachoud-Levi, A-C., Hantraye, P., Remy, P., 2006. Distribution of grey matter atrophy in Huntington's disease: a combined ROI and voxel-based morphometric study. NeuroImage 32, 1562-1575.

Eckert, T., Sailer, M., Kaufmann, J., Schrader, C., Peschel, T., Bodammer, N., Heinze, H-J., Schoenfeld, M.A., 2004. Differentiation of idiopathic Parkinson's

disease, multiple system atrophy, progressive supranuclear palsy and healthy controls using magnetisation transfer imaging. Neuroimage 21, 221-235.

ENIGMA, 2011. Genome-wide association meta-analysis of hippocampal volume: results from the ENIGMA consortium, Organization for Human Brain Mapping Meeting, June 2011, Quebec City, Canada
http://enigma.loni.ucla.edu/wpcontent/uploads/2011/01/EnigmaOHBMAbstract.pdf
Accessed 20 January 2011

Fields, H.L., Hjelmstad, G.O., Margolis, E.B., Nicola, S.M., 2007. Ventral tegmental area neurons in learned appetitive behaviour and positive reinforcement. Annual Review of Neuroscience 30, 289-316.

Filippi, L., Manni, C., Pierantozzi, M., Brusa, L., Danieli, R., Stanzione, P., Schillaci, O., 2006. 123I-FP-CIT in progressive supranuclear palsy in Parkinson's disease: a SPECT semiquantitative study. Nuclear Medicine Communications 27, 381-386.

Genovese, C.R., Lazar, N.A., Nichols, T., 2002. Thresholding of statistical maps in functional neuroimaging using the false discovery rate. NeuroImage 15, 870–878.

Gröschel, K., Hauser, T-K., Luft, A., Patronas, N., Dichgans, J., Litvan, I.B., Schulz, J.B., 2004 Magnetic resonance imaging-based volumetry differentiates progressive supranuclear palsy from corticobasal degeneration. NeuroImage 21, 701-704.

Haber, S.N., 2003. The primate basal ganglia: parallel and integrative networks. Journal of Chemical Neuroanatomy 26, 317-330.

Heimer, L., Van Hoesen, G.W., 2006. The limbic lobe and its output channels: implications for emotional function and adaptive behaviour. Neuroscience and Biobehavioral Reviews 30, 126-147.

Ikemoto, S., 2007. Dopamine reward circuitry: two projection systems from the ventral midbrain to the nucleus accumbens-olfactory tubercle complex. Brain Research Reviews 56, 27-78.

Josephs, K.A., Whitwell, J.L., Dickson, D.W., Boeve, B.F., Knopman, D.S., Petersen, R.C., Parisi, J.E., Jack Jr., C.R., 2008. Voxel based morphometryin autopsy proven PSP and CBD. Neurobiology of Aging 29, 280-289.

Josephs, K.A., Whitwell, J.L., Eggers, S.D., Senjem, M.L., Jack Jr., C.R., 2011. Gray matter correlates of behavioral severity in progressive supranuclear palsy. Movement Disorders DOI: 10.1002/mds.23471

Kvickström, P., Eriksson, B., van Westen, D., Lätt, J., Elfgren, C., Nilsson, C., 2011. Selective forntal neurodegeneration of the inferior fronto-occiptal fasciculus in progressive supranuclear palsy (PSP) demonstrated by diffusion tensor tractography. BMC Neurology 11, 13

Levitt, J.J., Styner, M., Niethammer, M., Bouix, S., Koo, M-S., Voglmaier, M.M., Dickey, C.C., Niznikiewicz, M.A., Kikinis, R., McCarley, R.W., Shenton, M.E., 2009. Shape abnormalities of caudate nucleus in schizotypal personality disorder. Schizophrenia Research 100, 127-139.

Levy, R., Ruberg, M., Herrero, M.T., Villares J., Havoy-Agid, F., Agid, Y., Hirsch, E.C., 1995. Alterations in GABAergic neurons in the basal ganglia of patients with progressive supranuclear palsy: An in-situ hybridization study of GAD_{67} messenger RNA. Neurology 45, 127-34.

Litvan, I., Bhatia, K.P., Burn, D.J., Goetz, C.G., Lang, A.E., McKeith, I., Quinn, N., Sethi, K.D., Shukts, C., Wenning, G.K., 2003. Movement Disorder Society Scientific Issues Report: SIC Task Force Appraisal of Clinical Diagnostic Criteria for Parkinsonian Disorders. Movement Disorders 18, 467-486.

Looi, J.C.L., Lindberg, O., Liberg, B.,Tatham, V., Kumar, R., Maller, J., Millard, E., Sachdev, P., Högberg, G., Pagani, M., Botes, L., Engman, E-L., Zhang, Y., Svensson, L., Wahlund, L-O., 2008. Volumetrics of the caudate nucleus: Reliability and validity of a new manual tracing protocol. Psychiatry Research: Neuroimaging 163, 279–288.

Looi J.C.L., Svensson L., Lindberg O., Zandbelt B.B., Östberg P., Örndahl E., Wahlund L-O., 2009. Putaminal volume in frontotemporal lobar degeneration and Alzheimer's Disease – differential volumes in subtypes of FTLD, AD, and controls. AJNR American Journal of Neuroradiology 30: 1552-1560.

Looi, J.C.L., Walterfang, M., Styner, M., Svensson, L., Lindberg, O., Östberg, P., Botes, L., Örndahl, E., Chua, P., Kumar, R., Velakoulis, D., Wahlund, L-O., 2010. Shape analysis of the neostriatum in frontotemporal lobar degeneration, Alzheimer's disease and controls. NeuroImage 51, 970-986.

Looi, J.C.L., Walterfang, M., Styner, M., Niethammer, M., Svensson, L., Lindberg, O., Östberg, P., Botes, L., Örndahl, E., Chua, P., Velakoulis, D., Wahlund, L-O., 2011. Shape analysis of the neostriatum in subtypes of frontotemporal lobar degeneration: neuroanatomically significant regional morphologic change. Psychiatry Research Neuroimaging 191, 98-111.

Madsen, S.K., Ho, A.J, Hua, X, Saharan, P.S., Toga, A.W., Jack Jr, C.R., Weiner, M.W., Thompson, P.M., ADNI, 2010. 3D maps localize caudate nucleus atrophy in 400 Alzheimer's disease, mild cognitive impairment and healthy elderly subjects. Neurobiology of Aging 31, 1312-1325.

Mann, D.M., Oliver, R., Snowden, J.S., 1993. The topographic distribution of brain atrophy in Huntington's disease and progressive supranuclear palsy. Acta Neuropathologica 85, 553 – 559.

Mazurová, Y., Rudolf, E., Látr, I., Österreicher, J., 2006. Proliferation and differentiation of endogenous neural stem cells in response to neurodegenerative response within the striatum. Neurodegenerative Disease 3, 12-18.

Oba, H., Yagishita, A., Terada, H., Barkovich, A.J,, Kutomi, K., Yamauchi, T,, Furui, S., Shimizu, T., Uchigata, M., Matsumura, K., Sonoo, M., Sakai, M., Takada, K., Harasawa, A., Takeshita, K., Kohtakem H., Tanaka, H., Suzuki, S., 2005. New and reliable MRI diagnosis for progressive supranuclear palsy. Neurology 64, 2050-2055.

Osaki, Y., Ben-Schlomo, Y., Lees, A.J., Daniel, S.E., Colosimo, C., Wenning, G.K., Quinn, N., 2004. Accuracy of clinical diagnosis of progressive supranuclear palsy. Movement Disorders 19, 181-189.

Oyanagi, K., Makifuchi, T., Ohtoh, T., Ikuta, F., Chen, K-M., Chase, T.N,, Gajdusek, D.C., 1994. Topographic investigation of brain atrophy in Parkinsonism-dementia complex of Guam: a comparison with Alzheimer's disease and progressive supranuclear palsy. Neurodegeneration 3, 301-304.

Padovani, A., Borroni, B., Brambati, S.M., Agosti, C., Broli, M., Alonso, R., Scifo, P., Belleli, D., Alberici, A., Gasparotti, R., Perani, D., 2006. Diffusion tensor imaging and voxel-based morphometry in early progressive supranuclear palsy. Journal of Neurology, Neurosurgery and Psychiatry 77, 457-463.

Quattrone, A., Nicoletti, G., Messina, D., Fera, F, Condino, F., Pugliese, F. Lanza, P., Barrone, P., Morgatnte, L., Zappio, M., Aguglia, U., Gallo, O., 2008. MR imaging index for differentiation of progressive supranuclear palsy from Parkinson disease and the Parkinson variant of multiple system atrophy. Radiology 246, 214-21.

Schrag, A., Good, C.D, Miszkiel, K., Morris, H.R., Mathias, M.D., Lees, A.J., Quinn, N.D., 2000. Differentiation of atypical parkinsonian syndromes with routine MRI. Neurology 54, 697-702.

Schulz, J.B., Skalej, M., Wedekind, D., Luft, A.R., Abele, M., Voigt, K., Dichgans, J., Klockgether, T., 1999. Magnetic resonance imaging–based volumetry differentiates idiopathic Parkinson's syndrome from multiple system atrophy and progressive supranuclear palsy. Annals of Neurology 45, 65-74.

Schwab R.S., England, A.C., 1969. Projection technique for evaluating surgery in Parkinson's disease. In Gillingham, F.J., Donaldson, I.M.L. (eds) Third symposium on Parkinson's disease. E & S Livingstone: Edinburgh, UK.

Seppi, K., Schocke, M.F., Esterhammer, R., Kremser, C., Brenneis, C., Mueller, J., Boesch, S., Jaschke, W., Poewe, W., Wenning, G.K., 2003. Diffusion-weighted imaging discriminates progressive supranuclear palsy from PD, but not from the parkinson variant of multiple system atrophy. Neurology 60, 922-927.

Sesack, S.R., Grace, A .A., 2010. Cortico-basal ganglia reward network: microcircuitry. Neuropsychopharmacology Reviews 35, 27-47.

Steele, J.C., Richardson, J.C., Olszewski, J., 1964. Progressive supranuclear palsy. A heterogeneous degeneration involving the brain stem, basal ganglia and cerebellum with vertical supranuclear gaze and pseudobulbar palsy, nuchal dystonia and dementia. Archives of Neurology 10, 333–59.

Styner, M., Oguz, I., Xu, S., Brechbuhler, C., Pantazis, D., Levitt, J.J., Shenton, M.E., Gerig, G., 2006. Framework for the statistical shape analysis of brain structures using SPHARM-PDM. Insight Journal 1–21.

Styner, M., Oguz, I., Xu, S., Pantazis, D., Gerig, G., 2007. Statistical group differences in anatomical shape analysis using the Hotelling T2 metric. Proc SPIE 6512, Medical Imaging 2007, pp 65123, z1-z11.

Thompson, D.W., 1945. On growth and form: a new edition. Cambridge University Press: New York, NY, USA.

Utter, A.A., Basso, M.A., 2008. The basal ganglia: an overview of circuits and function. Neurosci. Biobehav. Rev. 32, 333-342.

van Buren, J.M., 1963. Trans-synaptic retrograde degeneration in the visual system of primates. Journal of Neurology, Neurosurgery and Psychiatry 26, 402-409.

Walterfang, M., Looi, J.C.L., Styner, M., Danek, A., Niethammer, M., Walker, R., Evans, A., Koschet, K., Rodrigues, G., Hughes, A., Velakoulis, D., 2011. Shape alterations in the striatum in choreoacanthocytosis Psychiatry Research: Neuroimaging 192, 29-36.

Warren, N.M., Piggott, M.A., Greally, E., Lake, M., Lees, A.J., Burn, D.J., 2007. Basal ganglia cholinergic and dopaminergic function in progressive supranuclear palsy. Movement Disorders 22,1594–1600.

Williams, D.R., Lees, A.J., 2009. Progressive supranuclear palsy: clinicopathological concepts and diagnostic challenges. Lancet Neurology 8, 270-79.

Zaja-Milatovic, S., Milatovic, D., Schantz., A.M., Zhang, J., Montine, K.S., Samii, A., Deutch, A.Y., Montine, T.J., 2005. Dendritic degeneration in neostriatal medium spiny neurons in Parkinson disease. Neurology 64, 545-547.

Zaja-Milatovic, S., Keene, C.D., Montine, K.S., Leverenz, J.B., Tsuang, D., Montine, T.J., 2006. Selective dendritic degeneration of medium spiny neurons in dementia with Lewy bodies. Neurology 66, 1591-1593.

Table(s)

Table 1 - Participants

	Group	*n*	Mean (SD)	Difference (*P*-value)
Age at Study	PSP	15	67.8 (5.84)	0.873
	Control	15	68.2 (7.58)	
Gender	PSP (M:F)	8:7		0.796
	Controls (M:F)	9:6		0.439
ICV	PSP	15	1511.22 (247.98)	0.502
	Control	15	1462.38 (122.59)	

P-value from Independent Samples t-test, no assumption of equal variance; gender Chi-squared value based on equal proportions male and female, asymptotic significance value reported as *P*-Value; ICV = Intracranial Volume (cm^3); PSP = Progressive Supranuclear Palsy, SD = Standard deviation

Table 2 - Clinical data on PSP patients

Patient	Sex (M/F)	Age at MRI	S & E*	Dysexecutive	Apathy	Personality change
1	M	76	80	Y	Y	Y
2	M	64	20	Y	Y	Y
3	F	65	40	N	N	N
4	M	68	60	Y	N	Y
5	M	64	30	Y	N	Y
6	F	60	40	N	N	N
7	F	74	80	N	N	N
8	M	60	80	N	N	N
9	M	70	30	Y	N	N
10	M	70	80	N	N	N
11	M	80	40	Y	N	N
12	F	70	40	Y	N	Y
13	F	71	80	N	N	N
14	F	67	50	Y	Y	Y
15	F	60	70	Y	N	N

* Schwab and England disability scale (percentage), Dysexecutive: dysexecutive symptoms; Apathy: apathy/loss of initiative

Table 3: Between Group Differences – Striatal Volumes, Midbrain/Pons Area and Pons/Midbrain Ratio

	Caudate Volume	Putamen Volume	Midbrain Area	Pons Area	P/M ratio
PSP	5207 +/- 886	4735 +/- 708	93.8 +/- 20.1	525.5 +/- 61.6	5.77 +/- 0.8
Control	6305 +/- 886	5267 +/- 708	145.3 +/- 20.1	577.4 +/- 61.6	3.99 +/- 0.8
% difference	***-17%***	***-10%***	***-35%***	-9%	***45%***
P =	***0.002***	***0.024***	***< 0.001***	0.06	***< 0.001***

PSP = Progressive supranuclear palsy, +/- = Standard deviation, Volume measured in mm^3, Area measured in mm^2, % Difference = percentage difference of PSP estimated marginal mean compared to Control, Significant findings in bold italics.

Figure 1: **Mid-Sagittal view showing the penguin or Colibri silhouette of the midbrain and pons**

a) PSP patient

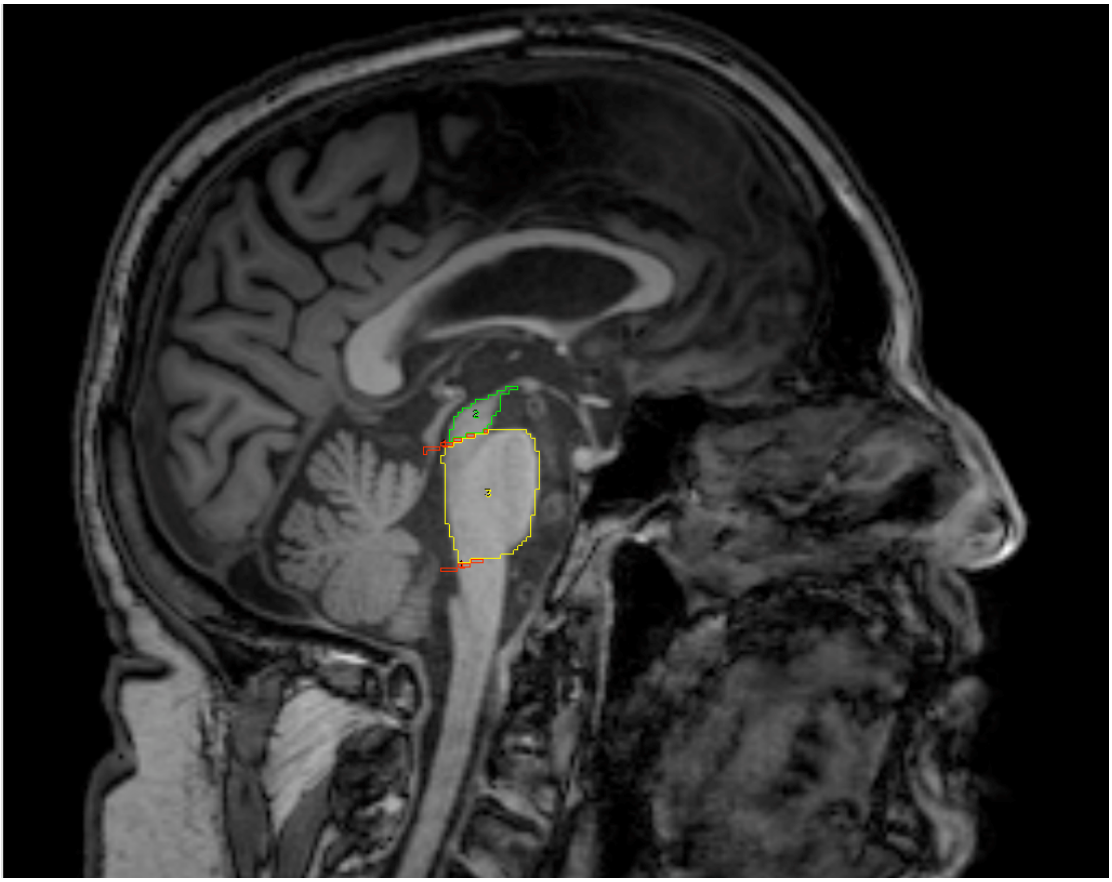

Superior red line = from superior pontine notch to inferior edge of quadrigeminal plate. Inferior red line = parallel to superior line, passing through inferior pontine notch. Both lines are partially obscured by object tracing in this image. Green area (“2”) = midbrain tracing, Yellow area (“3”) = pons tracing.

Note the “penguin” or Colibri silhouette of the midbrain and pons, characterized by the atrophic midbrain region, which appears as a “beak”.

b) Healthy Control

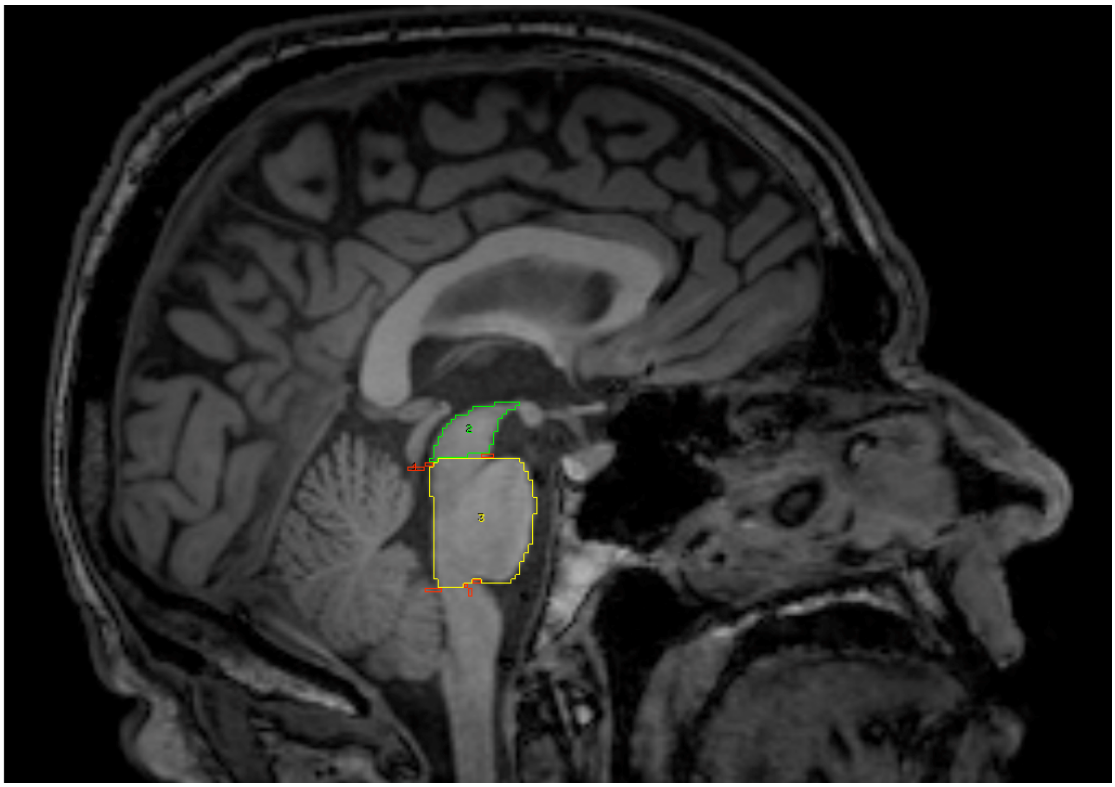

Red, green and yellow areas represent the same technique as Fig 1 a).

Note the more rotund “beak” comprising the midbrain, producing a broader “kookaburra” silhouette of the midbrain and pons.

Figure 2: Views of striatum traced using ANALYZE 10.0 software (control)

2a

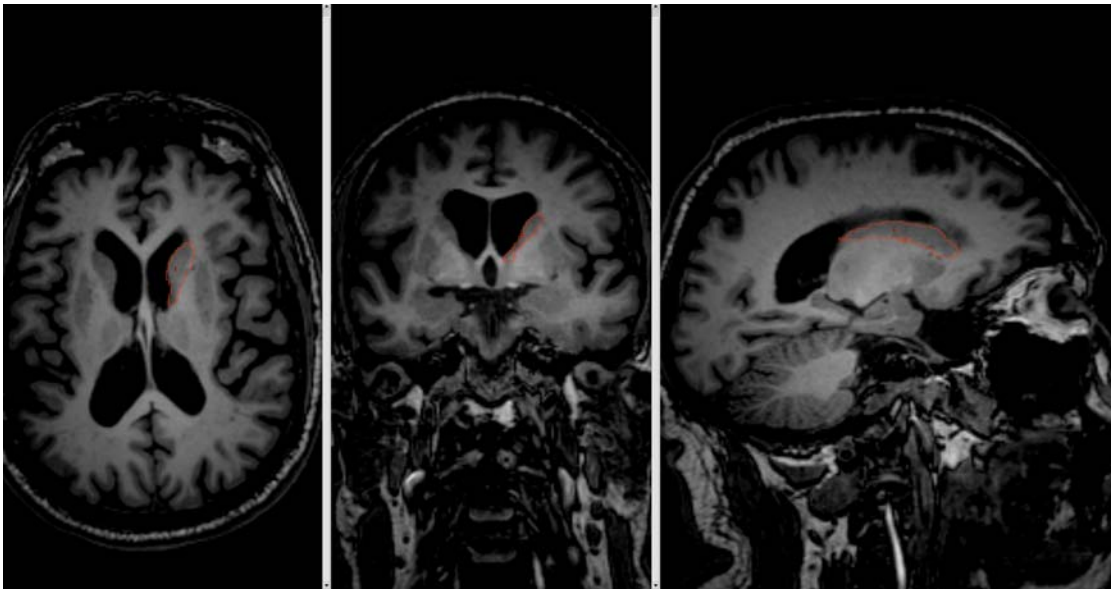

Axial, Coronal and Sagittal views, Caudate outlined in Red

2b

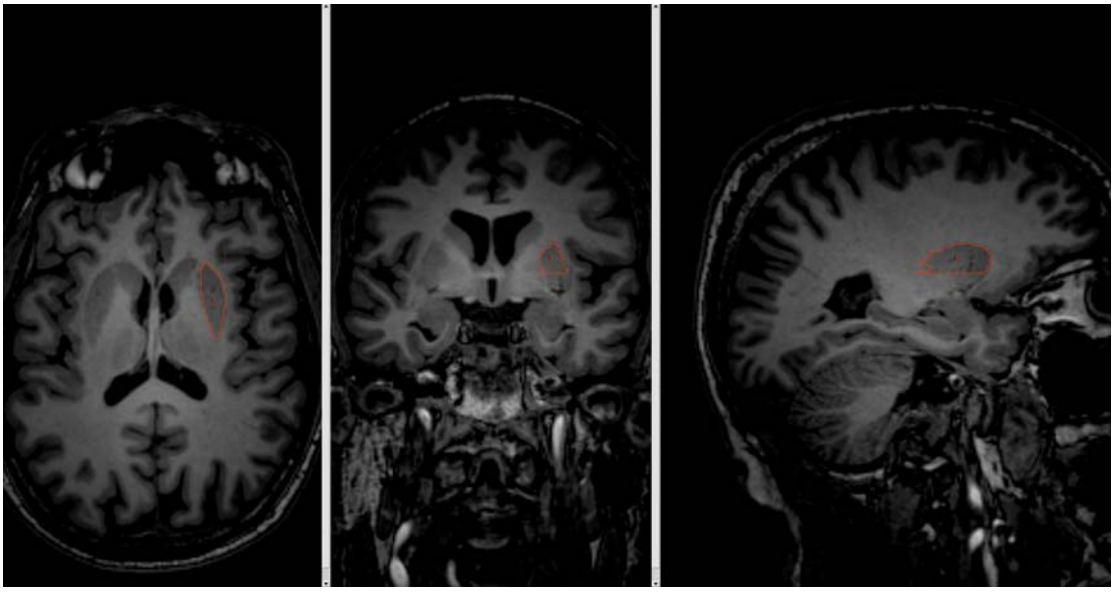

Axial, Coronal and Sagittal views, Putamen outlined in Red

Figure 3: Scatterplot of Bilateral Caudate and Putamen Volumes By Group

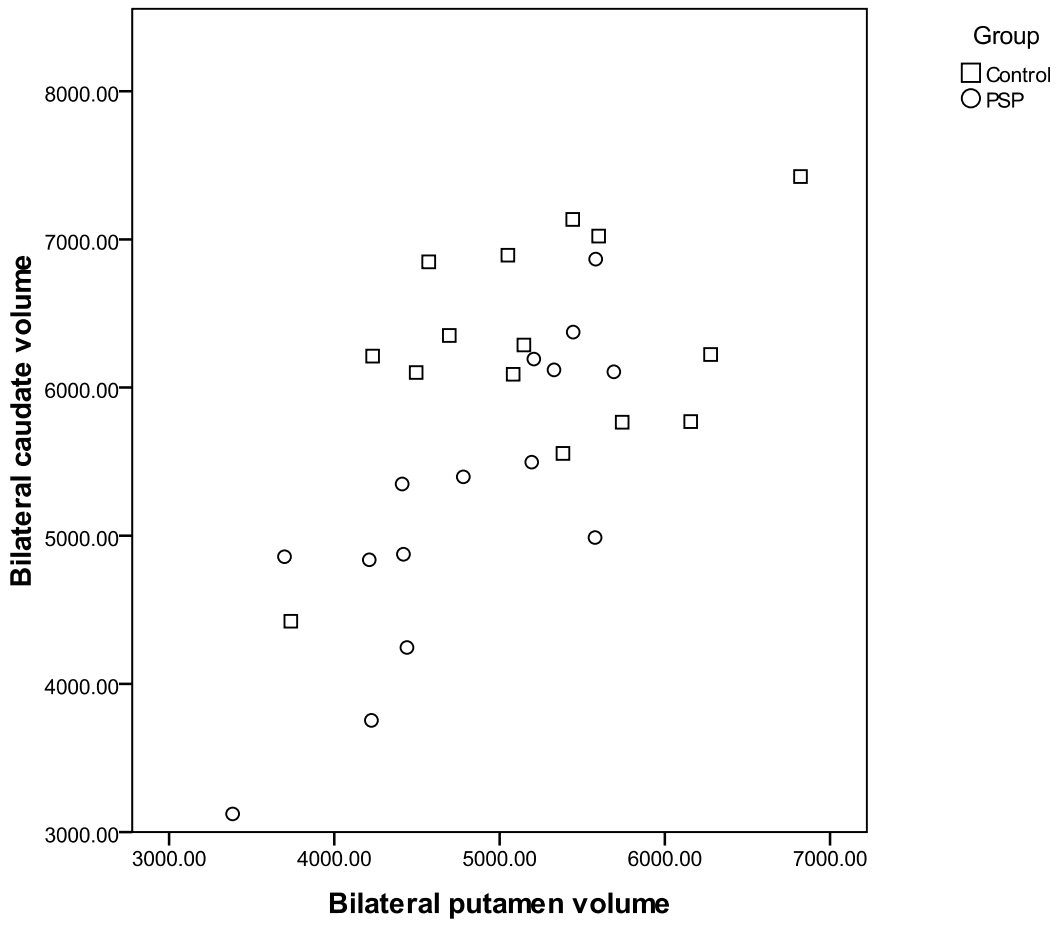

Volume in mm^3

Figure 4: Receiver-operating characteristics (ROC) curve of bilateral caudate volume for controls versus PSP

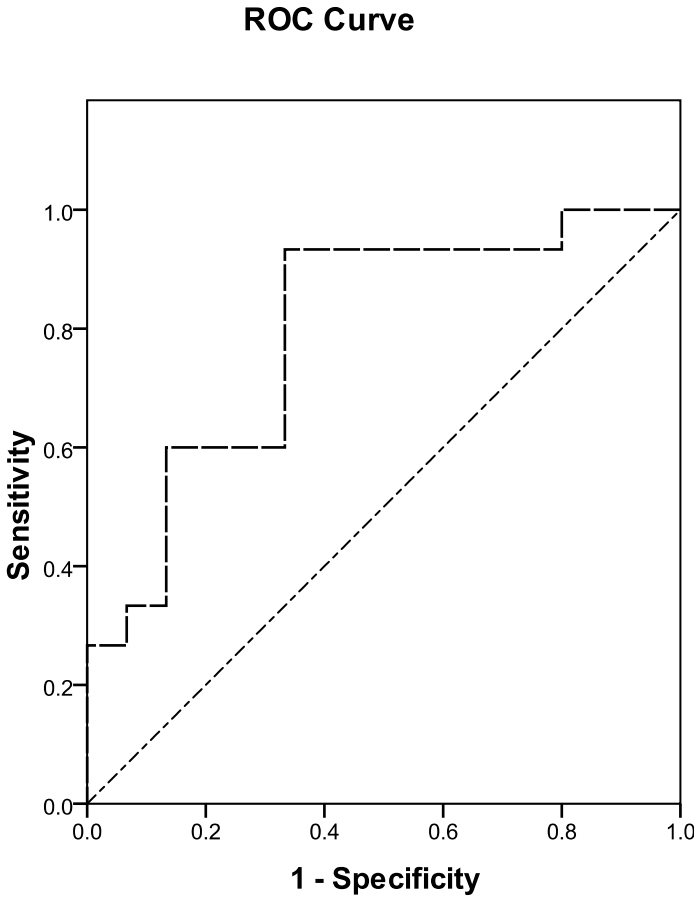

Diagonal (y=x) dotted line is a reference line

Figure 5: Scatterplot of Midbrain and Pons Areas By Group

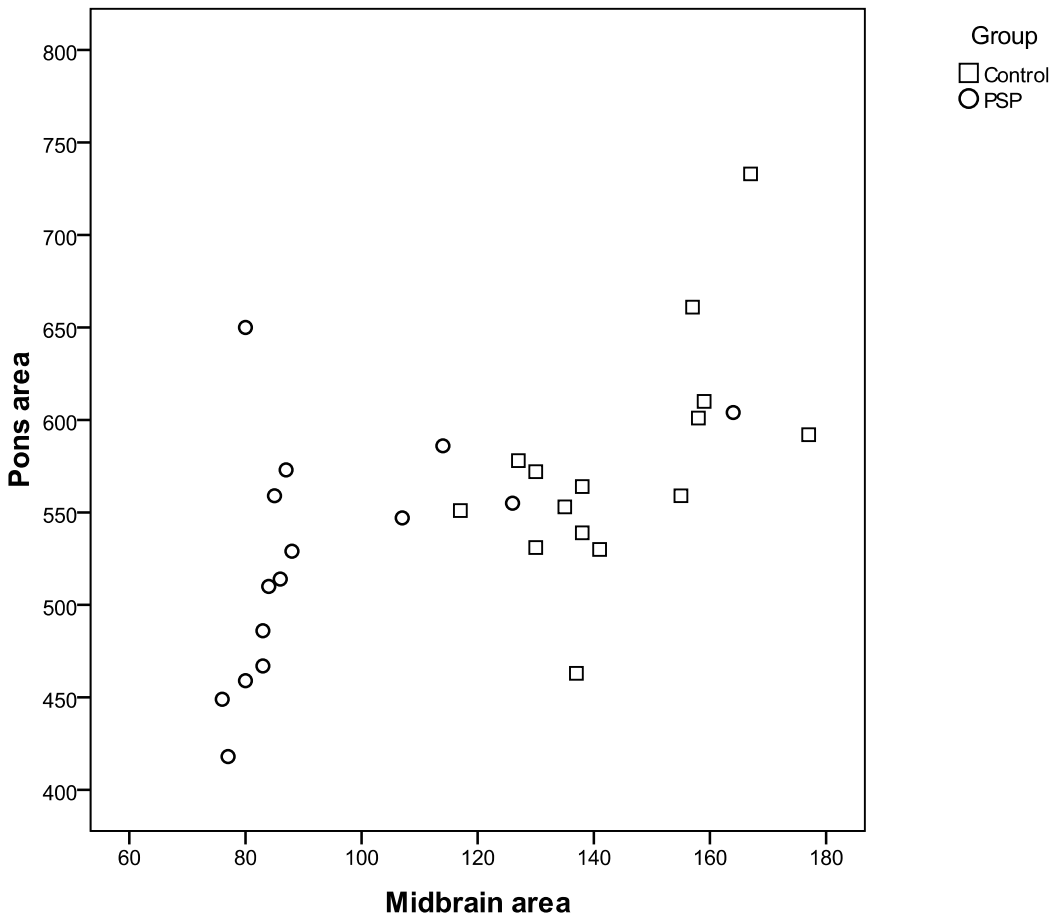

PSP: Progressive Supranuclear Palsy
Area in mm^2

Figure 6: Shape analysis of PSP versus Controls

LEFT CAUDATE

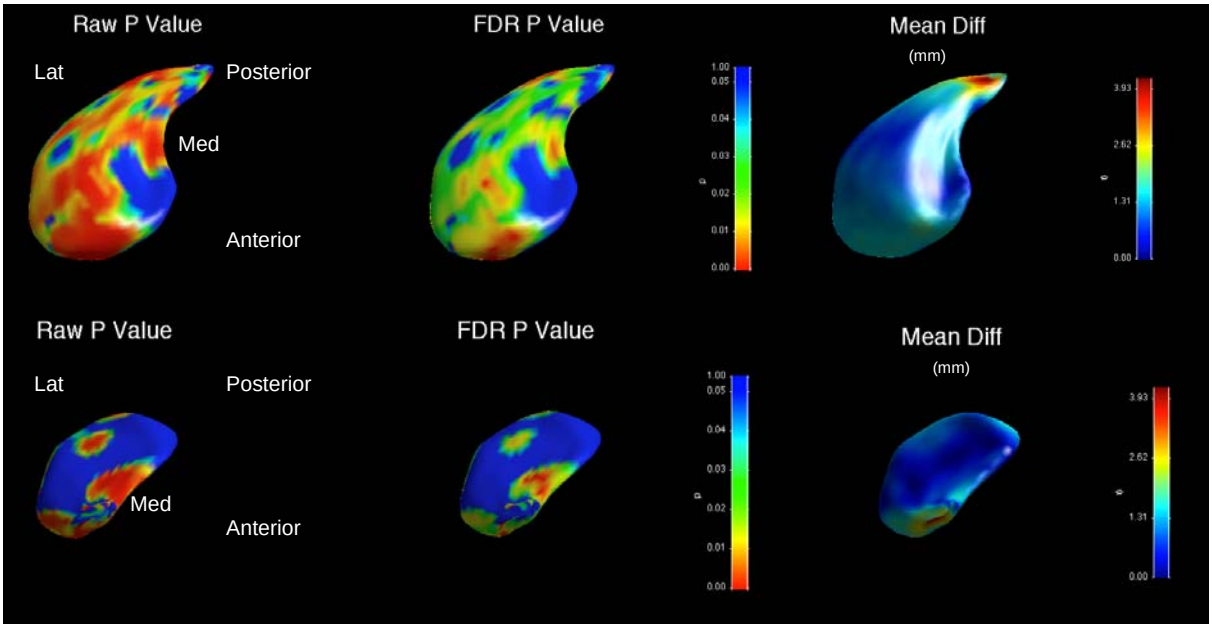

Dorsal aspect in top image, ventral aspect in bottom image
P of average statistic across surface: 0.0001

RIGHT CAUDATE

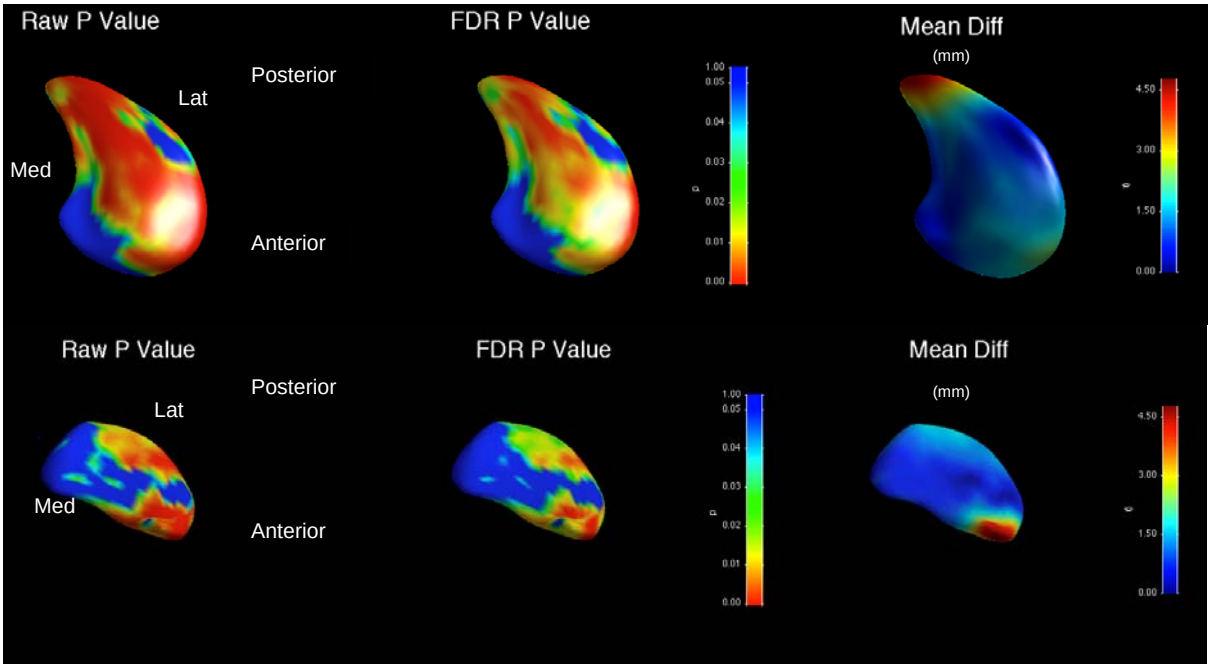

Dorsal aspect in top image, ventral aspect in bottom image
P of average statistic across surface: 0.0002

LEFT PUTAMEN

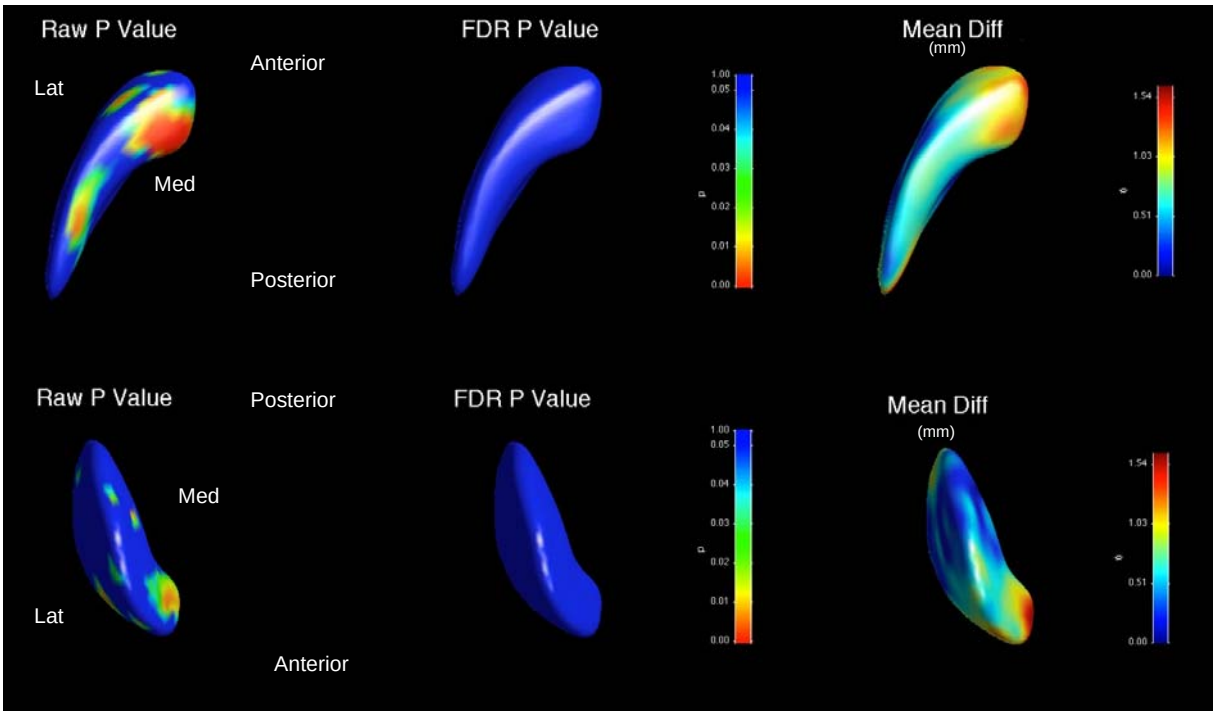

Dorsal aspect in top image, ventral aspect in bottom image
P value of average statistic across surface: 0.0174

RIGHT PUTAMEN

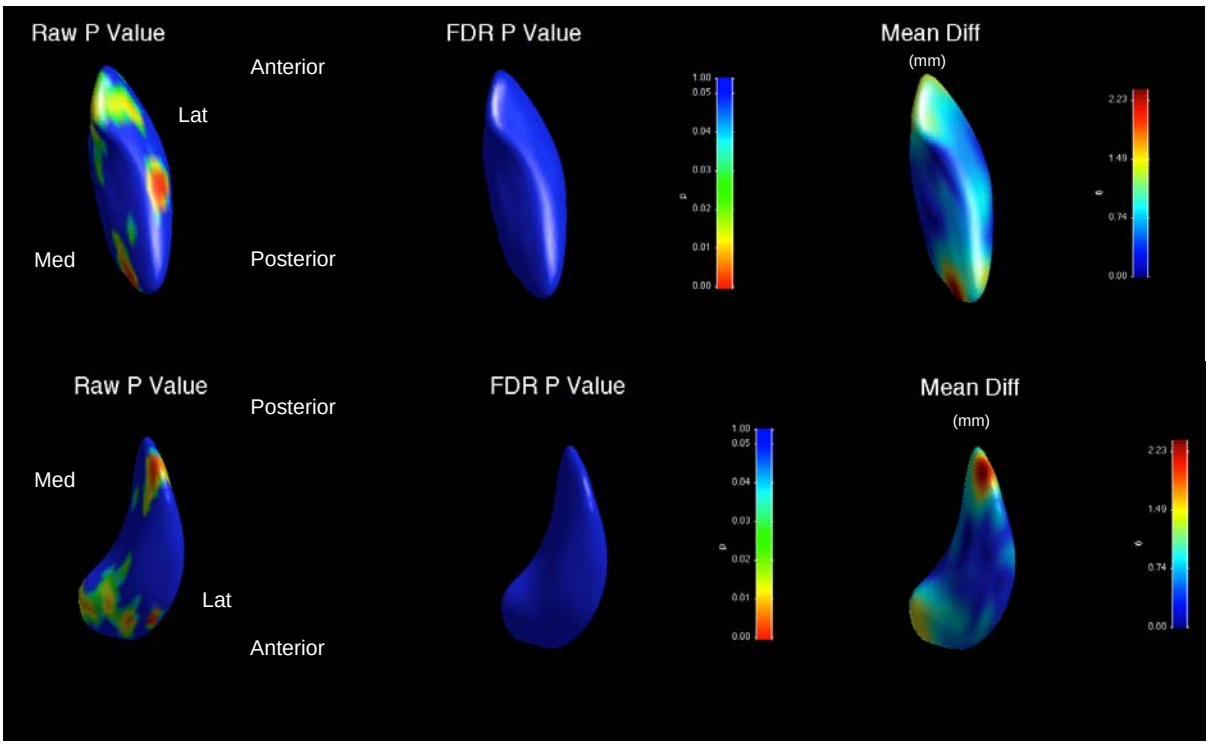

Dorsal aspect in top image, ventral aspect in bottom image
P value of average statistic across surface: 0.0169

Legend

PSP: Progressive supranuclear palsy
Lat: Lateral aspect
Med: Medial aspect
Anterior: rostral aspect
Posterior: caudal aspect

Global shape measures
The global shape measure describes the average Hotelling T^2 group difference metric across the whole surface of the caudate or putamen respectively, the single *P*-value displayed for each structure in Figure 6 is calculated by non-parametric permutation. On global shape measures, the bilateral neostriatum is significantly different in shape for PSP versus controls.

Shape measures: significance maps and displacement maps
For ease of reference, we present the data by structure (caudate or putamen), including the *p*-value shape significance maps and mean difference displacement maps. In the interests of brevity, we have displayed the mean difference magnitude displacement maps, including significance maps with significant findings.

***P* value of average statistic across surface**: is the comparison of the shape difference between PSP group and controls across the entire surface.

P-value significance maps
The *p*-value color significance scale is identical for all images, and warmer colors refer to smaller *p*-values less than 0.05, with the blue color corresponding to *p*-values above 0.05.

Raw P Value: Raw *P* value (as depicted by *P* value scale to the right of regional shape images) with warmer colors corresponding to smaller *P* values.

FDR P Value: False discovery rate *P* value (as depicted by *P* value scale to the right of regional shape images) with warmer colors corresponding to smaller *P* values.

Mean difference magnitude displacement maps
We have displayed volumes of deflation as positive values, such that the values represent millimetres of deflation of the overall larger structure compared to the smaller structure. This requires assignment of the 'nominal' larger structure for comparison and the group assigned as nominally larger was the control group (based upon the volumetric findings above). Thus, the values of deflation describe the degree of deflation of the PSP group compared to controls.

Additionally, the displacement direction was only in one direction in all analyses, without bi-directional shape changes. This was confirmed by using the visualizations of signed directional changes, which revealed unidirectional changes in all comparisons. Therefore, we used a unidirectional (non-signed) scale display.

Mean Diff: Mean difference magnitude displacement map of shape (scale: mm to right of map) with warmer colors corresponding to increased magnitude of deflation of shape of PSP group compared to controls). Note that the displacement color scale is unique for each image, and corresponds to the millimetres of deflation of the surface in that region; with warmer colors (such as red) corresponding to greater degrees of deflation, and cooler colors (such as blue) lesser degrees of deflation.

Figure 7 Striatal afferent connections

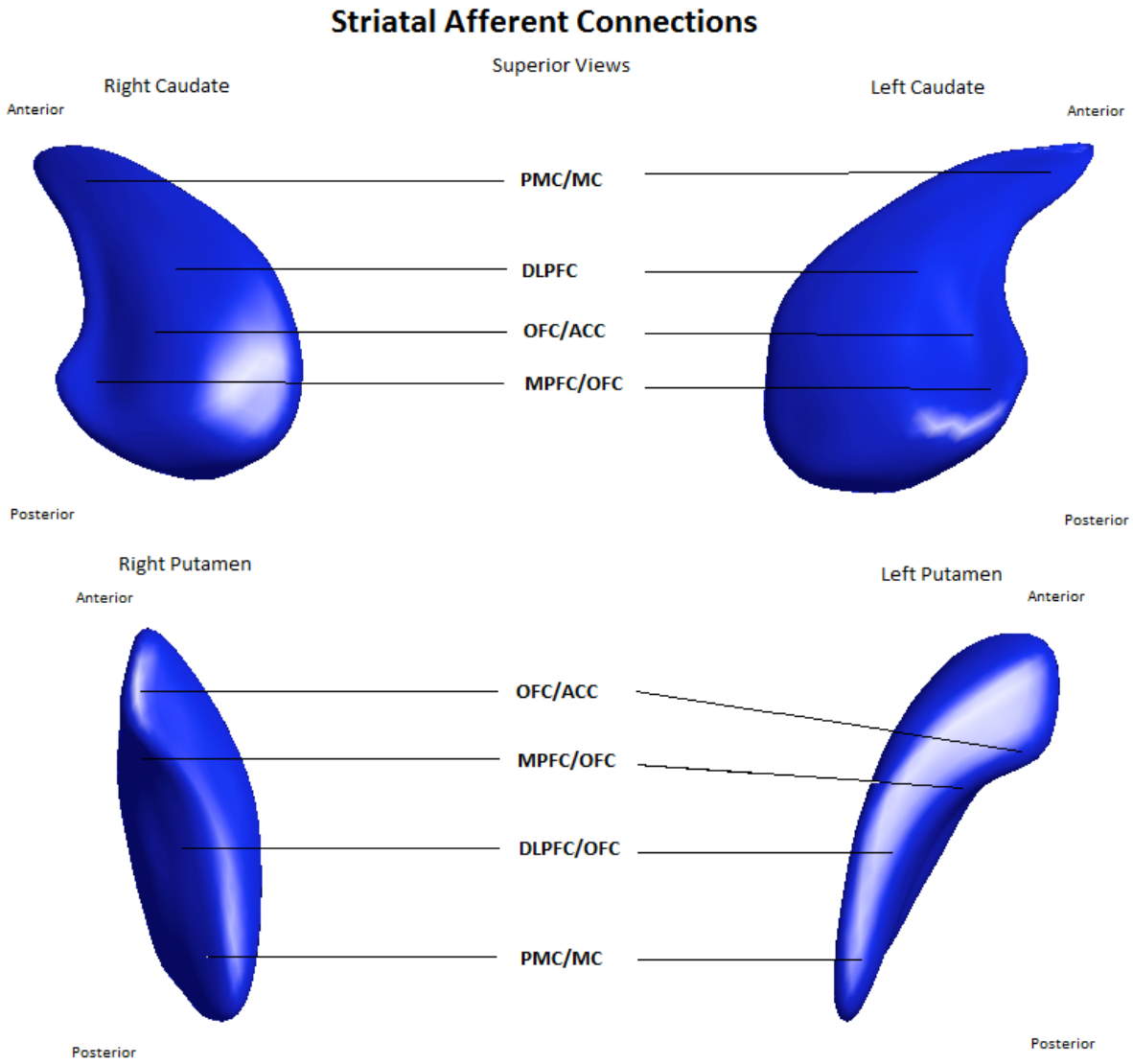

ACC = anterior cingulate gyrus, DLPFC = dorsolateral prefrontal cortex, MC = motor cortex, MPFC = medial prefrontal cortex, OFC = orbitofrontal cortex,PMC = premotor cortex

Striatal afferent connections compiled by the authors from Draganski et al., 2008; Haber, 2003; Utter and Basso, 2008.

Figure 8: Diagram of striatal afferent projections from frontal cortex

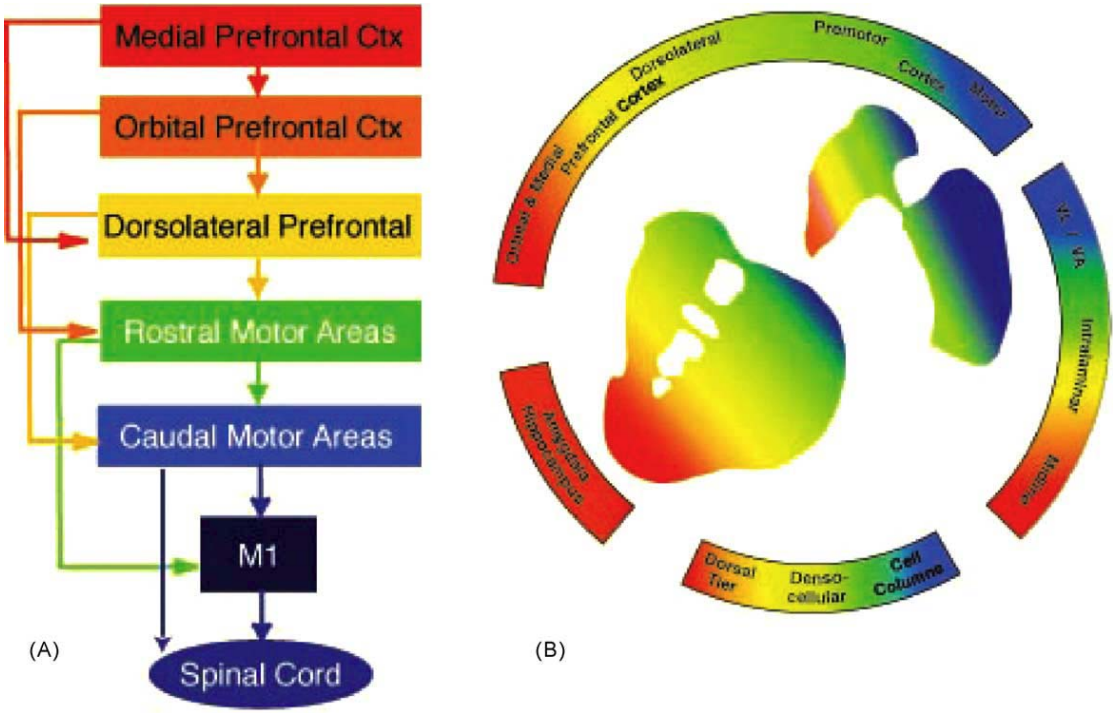

Fig. 8. Diagram demonstrating the functional organization of A. frontal cortex and B. striatal afferent projections. (A) Schematic illustration of the functional connections linking frontal cortical brain regions. (B) Organization of cortical and subcortical inputs to the striatum. In both (A) and (B), the colors denote functional distinctions. Blue: motor cortex, execution of motor actions; green: premotor cortex, planning of movements; yellow: dorsal and lateral prefrontal cortex, cognitive and executive functions; orange: orbital prefrontal cortex, goal-directed behaviors and motivation; red: medial prefrontal cortex, goal-directed behaviors and emotional processing. (Reproduced with permission from Haber, 2003, fig 3.)

Figure 9: Diagram of striatal afferent projections from cortex

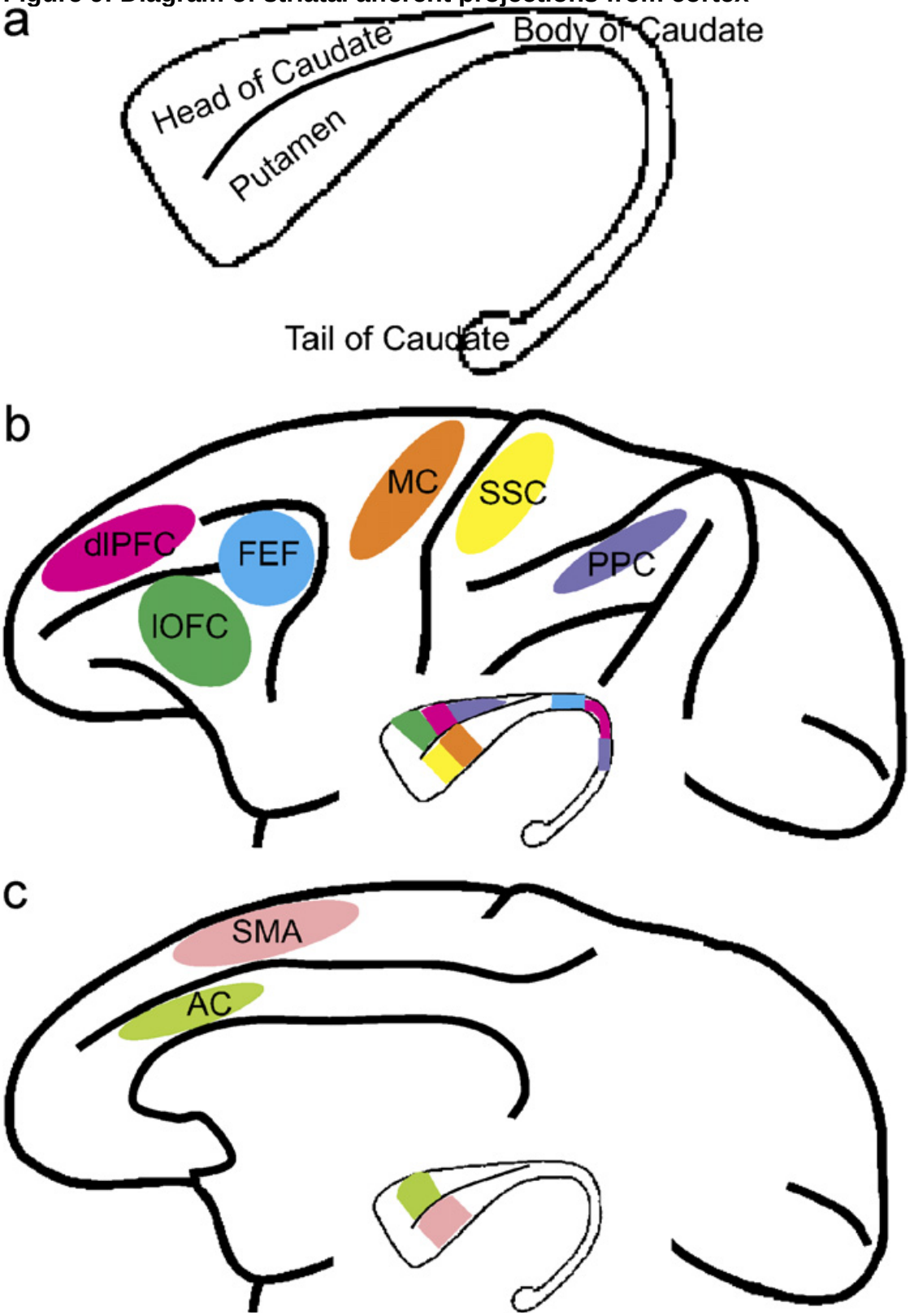

Fig. 9. Schematic showing anatomy of the striatum (a). Representative lateral (b) and medial (c) illustrations of cortical areas and their connections to the striatum. The colored segment in the striatum represents the area of the striatum receiving projections from the cortical area of the same color. Abbreviations: AC, anterior cingulate cortex; dlPFC, dorsal lateral prefrontal cortex; FEF, frontal eye field; lOFC, lateral orbitofrontal cortex; MC, motor cortex; PPC, posterior parietal cortex; SMA, supplementary motor area; SSC, somatosensory cortex.

Compiled from Alexander et al. (1986). (Reproduced with permission from Utter and Basso, 2008, Fig.2)

APPENDIX A: Computational Details of Group Comparisons, Error Corrections, Magnitude Displacement Maps

(Reproduced/adapted from Styner et al., 2006)

Group comparisons of shape

We calculate group differences by analyzing the spatial location of each point. For this option, no template is necessary and multivariate statistics of the (x,y,z) location is necessary. We have chosen to use the Hotelling T^2 two sample difference metric as a measurement of how 2 groups locally differ from each other. The standard Hotelling T^2 is defined as $T^2 = (\mu 1 - \mu 2)' (\Sigma (1 / n1 + 1 / n2))^{-1}(\mu 1 - \mu 2)$, where $\Sigma = (\Sigma_1(n1 - 1) + \Sigma_2(n2 - 1))/(n1 + n2 - 2)$ is the pooled covariance matrix. An alternative modified Hotelling T^2 metric is less sensitive to group differences of the covariance matrixes and the number of samples(Styner et al., 2007): $T 2 = (\mu 1 - \mu 2)'(\Sigma_1 1 / n1 + \Sigma_2 1 / n2)^{-1}(\mu 1 - \mu 2)$. All our current studies are based on this modified Hotelling T^2 metric.

We then want to test the two groups for differences in the means of the selected difference metric (univariate: Student t, multivariate: Hotelling T^2) at each spatial location. Permutation tests are a valid and tractable approach for such an application, as they rely on minimal assumptions and can be applied even when the assumptions of the parametric approach are untenable. Non-parametric permutation tests are exact, distribution free and adaptive to underlying correlation patterns in the data. Further, they are conceptually straightforward and, with recent improvements in computing power, are computationally tractable.

Our null hypothesis is that the distribution of the locations at each spatial element is the same for every subject regardless of the group. Permutations among the two groups satisfy the exchangeability condition, i.e. they leave the distribution of the

statistic of interest unaltered under the null hypothesis. Given n1 members of the first group a_k, k = 1 . . . n1 and n2 members of the second group b_k, k = 1 . . . n2, we can create M ≤((n1 + n2)!)/(n2!) permutation samples. A value of M from 20000 and up should yield results that are negligibly different from using all permutations.

Corrections for multiple comparisons

In this study, we are employing non-parametric permutation tests and false discovery rate as two alternative correction methods for the multiple comparison problem.

Correction for Type I Errors

The correction method for multiple comparisons is based on computing first the local p-values using permutation tests. The minimum of these p-values across the surface is then computed for every permutation. The appropriate corrected p-value at level α can then be obtained by the computing the value at the α-quantile in the histogram of these minimum values. Using the minimum statistic of the p-values, this method correctly controls for the family wise error rate, or the false positives, but no control of the false negatives is provided. The resulting corrected local significance values can thus be regarded as pessimistic estimates akin to a simple Bonferroni correction.

Correction for Type II Errors

Additionally to the non-parametric permutation correction, we have also implemented and applied a False Discovery Rate Estimation (FDR) method. The innovation of this procedure is that it controls the expected proportion of false positives only among those tests for which a local significance has been detected. The FDR method thus allows an expected proportion (usually 5%) of the FDR corrected significance values to be falsely positive. The correction using FDR provides an interpretable and adaptive criterion with higher power than the non-parametric permutation tests. FDR is further simple to implement and computationally efficient even for large datasets.

The FDR correction is computed as follows:

1. Select the desired FDR bound q, e.g. 5%. This is the maximum proportion of false positives among the significant tests that you are willing to tolerate (on average).

2. Sort the p-values smallest to largest.

3. Let p_q be the p-value for the largest index *i* of the sorted p-values $p_{sort,i} \leq q \cdot i/N$, where N is the number of vertices.

4. Declare all locations with a p-value $p \leq p_q$ significant.

Mean difference magnitude difference maps

These are calculated as the map of the absolute difference in the mean surfaces between groups (based upon the computations above), derived from the lengths of the difference vectors (that is the difference in vectors for analogous surface points between the groups).

References

Styner, M., Oguz, I., Xu, S., Brechbuhler, C., Pantazis, D., Levitt, J.J., Shenton, M.E., Gerig, G. 2006. Framework for the statistical shape analysis of brain structures using SPHARM-PDM. Insight J. 1–21.

Styner, M., Oguz, I., Xu, S., Pantazis, D., Gerig, G., 2007. Statistical group differences in anatomical shape analysis using the Hotelling T2 metric. Proc SPIE 6512, Medical Imaging 2007, pp 65123, z1-z11.

Appendix B: Receiver-operating characteristics curve for bilateral caudate and putamen volume

An ROC analysis was conducted to determine group membership based on bilateral caudate and bilateral putamen volume, showing that bilateral caudate volume of less than 4630 mm^3 predicted PSP membership versus control with a sensitivity of 0.933 and specificity 0.800, with area under the curve 0.796 +/- 0.084, asymptotic significance 0.006.

Area Under the Curve

Test Result Variable(s):BilatCaud

Area	Std. Error[a]	Asymptotic Sig.[b]	Asymptotic 95% Confidence Interval	
			Lower Bound	Upper Bound
.796	.084	.006	.632	.959

a. Under the nonparametric assumption

b. Null hypothesis: true area = 0.5

Coordinates of the Curve

Test Result Variable(s):BilatCaud

Positive if Greater Than or Equal To[a]	Sensitivity	1 - Specificity
3121.6900	1.000	1.000
3438.2000	1.000	.933
3999.7050	1.000	.867
4334.3000	1.000	.800
4630.1900	.933	.800
4847.9650	.933	.733
4866.8550	.933	.667
4931.4750	.933	.600
5168.5400	.933	.533
5373.3700	.933	.467
5446.8800	.933	.400
5525.9450	.933	.333

5660.7550	.867	.333
5768.3600	.800	.333
5930.0450	.733	.333
6095.3250	.667	.333
6103.7950	.600	.333
6112.8200	.600	.267
6155.8000	.600	.200
6202.3450	.600	.133
6217.6950	.533	.133
6255.0700	.467	.133
6319.2800	.400	.133
6362.8200	.333	.133
6611.1950	.333	.067
6857.3450	.267	.067
6879.8650	.267	.000
6957.7600	.200	.000
7078.3550	.133	.000
7279.2800	.067	.000
7425.1600	.000	.000

a. The smallest cutoff value is the minimum observed test value minus 1, and the largest cutoff value is the maximum observed test value plus 1. All the other cutoff values are the averages of two consecutive ordered observed test values.

Appendix C – Mesencephalic area, utility and possible significance of the Penguin Sign

Midbrain areas in the PSP group were significantly smaller than in controls (Table 1). Our average P/M ratio findings were 5.77 for PSP and 3.99 for controls, also representing a significant difference (Table 2). Quattrone et al. (2008) reported median P/M ratios of 6.67 for PSP and 3.85 for controls. Similar midbrain atrophy findings in PSP were obtained previously by Oba et al. (2005), using the inverse of the P/M ratio of midbrain-to-pons ratio, which we re-calculated as an average P/M ratio as 8.06 for their PSP group, and 4.22 for their controls. The differences between the studies may be explained by disease duration and clinical profile of the included subjects.

Table 1: Pons and Midbrain Mid-sagittal Area

Table 1a: MANCOVA Significance Results

Variable	Type III Sum of Squares	df	Mean Square	F	Sig.	Partial Eta Squared
Midbrain area	19911.948[a]	3	6637.316	16.205	.000	.652
Pons area	31496.738[c]	3	10498.913	2.805	.059	.245

Table 1b: MANCOVA Estimated Marginal Means

				95% Confidence Interval	
Variable	Group	Mean	Std. Error	Lower Bound	Upper Bound
Midbrain area	Control	145.266[a]	5.249	134.477	156.055
	PSP	93.801[a]	5.249	83.012	104.590
Pons area	Control	577.387[a]	15.866	544.774	609.999
	PSP	525.480[a]	15.866	492.868	558.093

a. Covariates appearing in the model are evaluated at the following values: Age at Study = 68.0000, ICV = 1486.8008.

PSP = Progressive supranuclear palsy, Area measured in mm^2

Table 2 – P/M Ratio in PSP and Control Group ANCOVA Estimated Marginal Means

Table 2a: ANCOVA Significance Results

Type III Sum of Squares	df	Mean Square	F	Sig.	Partial Eta Squared	Noncent. Parameter
23.838[a]	3	7.946	13.387	.000	.607	40.161

Table 2b ANCOVA Estimated Marginal Means

Dependent Variable:P/M ratio

Group	Mean	Std. Error	95% Confidence Interval	
			Lower Bound	Upper Bound
Control	3.993[a]	.200	3.582	4.403
PSP	5.769[a]	.200	5.358	6.180

a. Covariates appearing in the model are evaluated at the following values: Age at Study = 68.0000, ICV = 1486.8008.

PSP = Progressive supranuclear palsy, Volume measured in mm^3

Calculating a receiver operating characteristics curve for P/M ratio to predict a diagnosis of PSP, we found a cut-off of 4.63 yielded 86.7% sensitivity and 93.3% specificity, which is similar to a value of 4.65 proposed previously (Quattrone et al., 2008). The area under the curve was 0.936+/-0.054, with asymptotic significance $P<0.001$.

Figure : Receiver operating characteristics curve for P/M ratio predicting PSP

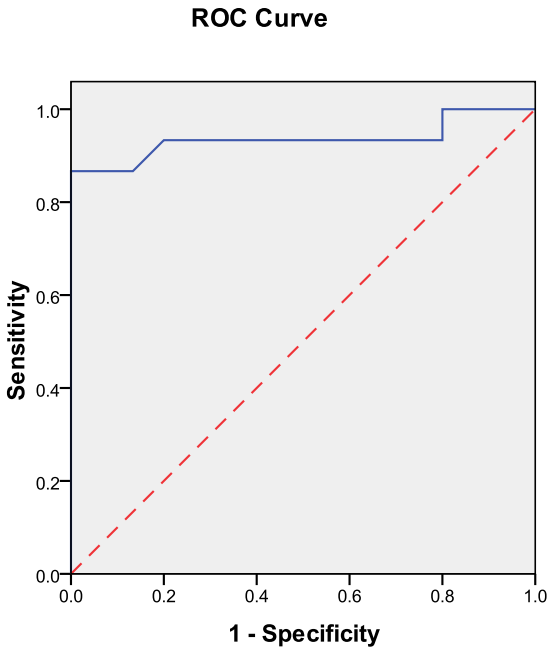

Dotted red line: random guess line
Solid blue line: ROC for pons/midbrain ratio predicting diagnosis of PSP

Area Under the Curve

Test Result Variable(s):P/M ratio

Area	Std. Error[a]	Asymptotic Sig.[b]	Asymptotic 95% Confidence Interval	
			Lower Bound	Upper Bound
.936	.054	.000	.000	1.000

The test result variable(s): P/M ratio has at least one tie between the positive actual state group and the negative actual state group. Statistics may be biased.

a. Under the nonparametric assumption

b. Null hypothesis: true area = 0.5

Coordinates of the Curve

Test Result Variable(s):P/M ratio

Positive if Greater Than or Equal To[a]	Sensitivity	1 - Specificity
2.3400	1.000	1.000
3.3600	1.000	.933
3.4950	1.000	.867
3.6450	1.000	.800
3.7200	.933	.800
3.7800	.933	.733
3.8200	.933	.667
3.8750	.933	.600
3.9950	.933	.533
4.0850	.933	.467
4.0950	.933	.400
4.1550	.933	.333
4.3000	.933	.267
4.3950	.933	.200
4.4750	.867	.133
4.6300	.867	.067
4.9100	.867	.000
5.1250	.800	.000
5.2850	.733	.000
5.5300	.667	.000

5.6850	.600	.000
5.8000	.533	.000
5.8850	.467	.000
5.9450	.400	.000
5.9950	.333	.000
6.0400	.267	.000
6.3250	.200	.000
6.5850	.133	.000
7.3575	.067	.000
9.1250	.000	.000

The test result variable(s): P/M ratio has at least one tie between the positive actual state group and the negative actual state group.

a. The smallest cutoff value is the minimum observed test value minus 1, and the largest cutoff value is the maximum observed test value plus 1. All the other cutoff values are the averages of two consecutive ordered observed test values.

Mesencephalic atrophy in PSP may have a number of clinical implications. The ventral tegmental area (VTA) has efferent dopaminergic excitatory and afferent inhibitory projections chiefly to and from the nucleus accumbens, prefrontal cortex, amygdala and the ventral pallidum (Fields et al., 2007). Most directly, meso-cortical disruption may impact upon habit formation, goal-directed behaviour and investigatory behaviour (Ikemoto, 2007). Thus, VTA atrophy may impact adversely on frontostriatal circuits in particular, resulting in apathy, obsessive-compulsive behaviour and executive dysfunction. Conversely, the nucleus accumbens projects inhibitory fibers to the substantia nigra, and thence to the mediodorsal thalamus which projects excitatory fibers to the prefrontal cortex (Sesack and Grace, 2010). Accordingly, substantia nigra atrophy may further result in release of inhibition of the mediodorsal thalamus, and thus excitation of prefrontal cortex, perhaps resulting in utilization or obsessive-compulsive behaviors. The overall effect of marked VTA

atrophy in PSP combined with caudate atrophy may be to dampen goal-directed behavior and perhaps lessen relative the propensity to obsessive-compulsive behaviors and stereotypies in contrast to primarily neostriatal disorders, such as Huntington's disease and perhaps frontotemporal lobar degeneration.

Also relevant to neostriatal and mesencephalic atrophy is evidence that long-term potentiation and long-term depression representing plasticity in the basal ganglia may result in clinical manifestations in neurodegenerative disease through structural changes effecting further functional, and hence, via plasticity, structural change (Berretta et al., 2007).

References

Berretta, N., Nistico, R., Bernardi, G., Mercuri, N.B. 2007. Synaptic plasticity in the basal ganglia: a similar code for physiological and pathological conditions. Progress in Neurobiology 84, 343-362.

Fields, H.L., Hjelmstad, G.O., Margolis, E.B., Nicola, S.M. 2007. Ventral tegmental area neurons in learned appetitive behaviour and positive reinforcement. Ann Rev Neurosci 30, 289-316.

Ikemoto, S. 2007. Dopamine reward circuitry: two projection systems from the ventral midbrain to the nucleus accumbens-olfactory tubercle complex. Brain Research Reviews 56, 27-78.

Oba, H., Yagishita, A., Terada, H., Barkovich, A.J,, Kutomi, K., Yamauchi, T,, Furui, S., Shimizu, T., Uchigata, M., Matsumura, K., Sonoo, M., Sakai, M., Takada, K.,

Harasawa, A., Takeshita, K., Kohtakem H., Tanaka, H., Suzuki, S. 2005. New and reliable MRI diagnosis for progressive supranuclear palsy. Neurology 64, 2050-2055.

Quattrone, A., Nicoletti, G., Messina, D., Fera, F, Condino, F., Pugliese, F. Lanza, P., Barrone, P., Morgatnte, L., Zappio, M., Aguglia, U., Gallo, O. 2008. MR imaging index for differentiation of progressive supranuclear palsy from Parkinson disease and the Parkinson variant of multiple system atrophy. *Radiology* 246, 214-21.